Trends, composition, and sources of carbonaceous aerosol at the Birkenes Observatory, Northern Europe, 2001-2018

Karl Espen Yttri[1], Francesco Canonaco[2,7], Sabine Eckhardt[1], Nikolaos Evangeliou[1], Markus Fiebig[1], Hans Gundersen[1], Anne-Gunn Hjellbrekke[1], Cathrine Lund Myhre[1], Stephen Matthew Platt[1], André S. H. Prévôt[2], David Simpson[3,4], Sverre Solberg[1], Jason Surratt[5], Kjetil Tørseth[1], Hilde Uggerud[1], Marit Vadset[1], Xin Wan[6], and Wenche Aas[1]

[1] NILU - Norwegian Institute for Air Research, P.O. Box 100, N-2027 Kjeller, Norway

[2] Paul Scherrer Institute (PSI), 5232 Villigen-PSI, Switzerland

[3] EMEP MSC-W, Norwegian Meteorological Institute, Oslo, Norway

[4] Department of Earth & Space Sciences, Chalmers Univ. Technology, Gothenburg, Sweden

[5] Department of Environmental Sciences & Engineering, University of North Carolina

[6] Key Laboratory of Tibetan Environment Changes and Land Surface Processes, Institute of Tibetan Plateau Research, Chinese Academy of Sciences Courtyard 16, Lin Cui Road, Chaoyang District, Beijing 100101, P.R. China

[7] Datalystica Ltd., 5234 Villigen, Switzerland

To whom correspondence should be addressed: Karl Espen Yttri, e-mail address: key@nilu.no

Abstract

We present 18 years (2001–2018) of aerosol measurements: organic and elemental carbon (OC and EC), organic tracers (levoglucosan, arabitol, mannitol, trehalose, glucose, 2-methyltetrols), trace elements and ions at the Birkenes Observatory (Southern Norway), a site representative of the Northern European region. The OC/EC (2001–2018) and the levoglucosan (2008–2018) time series are the longest in Europe, with OC/EC available for the PM_{10}, $PM_{2.5}$ (fine) and $PM_{10-2.5}$ (coarse) size fractions, providing the opportunity for a nearly two-decade long assessment. Using positive matrix factorization (PMF) we identify seven carbonaceous aerosol sources at Birkenes: Mineral dust dominated (MIN), traffic/industry-like (TRA/IND), short range transported biogenic secondary organic aerosol ($BSOA_{SRT}$), primary biological aerosol particles (PBAP), biomass burning (BB), ammonium nitrate dominated (NH_4NO_3), and (one low carbon fraction) sea salt (SS).

We observed significant ($p<0.05$), large decreases of EC in PM_{10} (-3.9% yr^{-1}) and $PM_{2.5}$ (-4.2% yr^{-1}), and a smaller decline in levoglucosan (-2.8% yr^{-1}), suggesting that OC/EC from traffic and industry is decreasing, while abatement of OC/EC from biomass burning has been slightly less successful. EC abatement of anthropogenic sources is further supported by decreasing EC fractions in $PM_{2.5}$ (-3.9% yr^{-1}) and PM_{10} (-4.5% yr^{-1}). PMF apportioned 72% of EC to fossil fuel sources, further supported by PMF applied to absorption photometer data, which yielded a two-factor solution with a low aerosol Ångstrøm

1

exponent (AAE=0.93) fraction assumed to be equivalent black carbon from fossil fuel combustion (eBC$_{ff}$), contributing 78% to eBC mass. The higher AAE fraction (AAE=2.04) is likely eBC from BB (eBC$_{bb}$). Source receptor model calculations (FLEXPART) showed that Continental Europe and western Russia were the main source regions both of elevated eBC$_{bb}$ and eBC$_{ff}$.

Dominating biogenic sources explain why there was no downward trend for OC. A relative increase in the OC fraction in PM$_{2.5}$ (+3.2% yr^{-1}) and PM$_{10}$ (+2.3% yr^{-1}) underscores the importance of biogenic sources at Birkenes (BSOA and PBAP), which were higher in the vegetative season and dominated both fine (53%) and coarse (78%) OC. Furthermore, 77–91% of OC in PM$_{2.5}$, PM$_{10-2.5}$ and PM$_{10}$ was attributed to biogenic sources in summer vs. 22-37% in winter. The coarse fraction had the highest share of biogenic sources regardless of season and was dominated by PBAP, except in winter.

Our results show a shift in aerosol composition at Birkenes and thus also in the relative source contributions. The need for diverse off-line and on-line carbonaceous aerosol speciation to understand carbonaceous aerosol sources, including their seasonal, annual, and long-term variability has been demonstrated.

1. Introduction

Carbonaceous aerosol has been studied intensively over the last 20 years due to its influence on radiative forcing (Bond et al., 2013; Myhre and Samset, 2015; Lund et al., 2018), both directly by scattering and absorption of sunlight, and semi directly and indirectly by influencing cloud properties (Boucher et al., 2013; Hodnebrog et al., 2014; Myhre et al., 2013). It also contributes to the burden of respiratory and cardiovascular disease (Janssen et al., 2012; WHO, 2013). Consequently, carbonaceous aerosol [here: elemental carbon (EC) and organic carbon (OC)] is measured regularly in major air monitoring networks such as e.g., EMEP and IMPROVE (e.g., Malm et al. 1994; Tørseth and Hov, 2003; Tørseth et al., 2012; UNECE, 2019; Hjellbrekke, 2020). Carbonaceous aerosol has an atmospheric lifetime of days to a few weeks and is thus relevant for atmospheric long-range transport. Accordingly, the European Monitoring and Evaluation Programme (EMEP) included OC/EC measurements in 2004 after a pioneering measurement campaign at 12 European sites from 2002–2003 (Yttri et al., 2007a; Tørseth et al., 2012), showing that carbonaceous aerosol was a major constituent of the ambient aerosol in the European rural background environment, accounting for 9–37% (OM = organic matter) and 1–5% (EC) of PM$_{10}$, and that OM was more abundant than sulfate (SO$_4^{2-}$) at sites reporting both variables (Yttri et al., 2007a). Similar conclusions were found from another long-term campaign, CARBOSOL (Gelencsér et al., 2007; Pio et al., 2007), which monitored atmospheric aerosol and its components for two years at six sites along a west-east transect extending from the Azores, in the mid-Atlantic Ocean, to K-Kuszta (Hungary), in centra Europe.

There are numerous carbonaceous aerosol sources, both anthropogenic, e.g. emissions from combustion of fossil fuel and biomass, and biogenic, e.g. vegetation emitted terpene/isoprene oxidation,

73   and primary biological aerosol particles (PBAP) from e.g. plants and fungi (Bauer et al., 2002; Donahue

74   et al., 2009; Hallquist et al., 2009; Fröhlich-Nowoisky et al., 2016).

75   Detailed source apportionment and quantification of carbonaceous aerosol is challenging due to

76   it numerous sources, the complexity of atmospheric formation and the vast number of organic

77   compounds associated with carbonaceous aerosols. A few studies have addressed carbonaceous aerosol

78   sources in the European rural background environment using source-specific organic tracers (Gelencsér

79   et al., 2007; Szidat et al., 2009; Genberg et al., 2011; Gilardoni et al., 2011; Yttri et al., 2011a,b). These

80   consistently show that residential wood burning dominates OC in winter, whereas biogenic secondary

81   organic aerosol (BSOA) is the major source in summer. PBAP makes a significant contribution to PM_{10}

82   in the vegetative season in the Nordic countries, second only to BSOA (Yttri et al., 2011a,b). Fossil fuel

83   sources typically dominate EC regardless of season but residential wood burning emissions can be

84   equally important and occasionally dominate in the heating season (Zotter et al., 2014; Yttri et al., 2019).

85   On-line high time-resolution measurements by aerosol mass spectrometer (AMS) and aerosol chemical

86   speciation monitors (ACMS) have become available in recent years, complementing off-line analysis of

87   organic tracers. In the comprehensive study by Crippa et al. (2014), including 15 European rural

88   background sites and 2 urban sites, covering winter, spring and fall, hydrocarbon-like organic aerosol

89   (OA) (11±5%) and biomass burning OA (12±5%) contributed almost equally to the total OA

90   concentration. The vast majority was however attributed to secondary sources; i.e., semi volatile

91   oxygenated OA (34±11%) and low-volatility oxygenated OA (50±16%). Secondary oxygenated OA

92   (OOA) can be both anthropogenic and biogenic; however Crippa et al. (2014) did not draw any

93   conclusions on this. Results presented by Bougiatioti et al. (2014) show how freshly emitted biomass

94   burning OA can be transformed to more oxidized OOA after just a short time in the atmosphere when

95   subject to high temperatures and high solar radiation.

96   Over the last decades, European anthropogenic emissions of secondary inorganic aerosol precursors,

97   e.g. ammonia (NH_3) and nitrogen oxides (NO_x), and non-methane volatile organic compounds

98   (NMVOC) have stabilized, and those of sulfur dioxide (SO_2) significantly reduced, following

99   implementation of the Gothenburg Protocol (Reis et al., 2012; UNECE, 2013; Matthews et al., 2020).

100   The anthropogenic carbonaceous aerosol is not regulated by any binding international protocol, although

101   co-benefit is expected from the regulation of NO_X and NMVOC, which act as precursors of secondary

102   organic aerosol (Hallquist et al., 2009). $PM_{2.5}$ was included in the revised version of the Gothenburg

103   protocol (UNECE, 2013) in 2012, which states that effort should be directed towards sources that also

104   emit black carbon (BC), which inevitably also will influence OC.

105   Residential wood burning is a major source of carbonaceous aerosol in circumpolar countries (e.g.

106   Yttri et al., 2014) and even considered the most important source in Norway, accounting for 48% (2017)

107   of $PM_{2.5}$ (Grythe et al., 2019). This region also regularly experiences major wild and agricultural fires

108   (e.g. Stohl et al., 2006 and 2007). A growing number of studies show that residential wood burning is

more widespread in continental Europe than previously assumed and that its contribution to the ambient carbonaceous aerosol can be substantial (Sillanpää et al., 2005; Gelencsér et al., 2007; Puxbaum et al., 2007; Lanz et al., 2010; Maenhaut et al., 2012; Genberg et al., 2011; Fuller et al., 2014; Yttri et al., 2019) and even dominating (Szidat et al., 2007; Herich et al., 2014). Residential wood burning is a decentralized source in Europe and combustion typically takes place in small units where the emissions are emitted without after-treatment. An economic downturn in Greece compelled households to burn firewood and waste material as fuel costs rose, increasing residential wood burning emissions in urban areas by 30% (Saffari et al., 2013). Future increases in European wood burning emissions might occur due to climate change mitigation policies supporting the use of renewable and biofuels (van der Gon et al., 2015). Denier van der Gon et al. (2015) conclude that European emissions from residential wood burning are significantly underestimated, thus it appears timely to address how ambient carbonaceous aerosol -particularly from biomass burning -has developed over the last two decades.

Kahnert et al. (2004) and Tørseth et al. (2012) highlight the importance of long-term measurements (> 10 years) of carbonaceous aerosol. The Birkenes Observatory in southern Norway holds the longest time series of OC and EC in Europe, dating back to 2001, including measurements in both the PM_{10} and the $PM_{2.5}$ fractions. Influenced by major anthropogenic emission regions in Europe, the Birkenes Observatory is well suited to monitor air pollution from Continental Europe.

Here we apply positive matrix factorization (PMF) to identify sources of carbonaceous aerosol at the Birkenes Observatory. Measurements of complementary species accompany OC/EC monitoring, allowing us to understand these sources, their contribution and variability at time scales from minutes to decades: organic tracers for biomass burning (levoglucosan), PBAP (arabitol, mannitol, trehalose and glucose) and BSOA (2-methyltetrols), as well as high time resolution equivalent black carbon resulting from biomass (eBC_{bb}) and fossil (eBC_{ff}) fuel combustion, derived from multiwavelength aethalometer measurements.

2. Methodology

2.1 Sampling site

The Birkenes Observatory (58°23'N, 8°15'E, 219 m above sea level, asl) is an EMEP/GAW (Global Atmospheric Watch) supersite in southern Norway (Figure 1) situated 100 m south-east of the old Birkenes site, initiating measurements in 2009. The observatory is in the Boreo-nemorale zone with mixed coniferous and deciduous trees (65% of the land use near the site); the remainder being meadows (10%), low intensity agricultural areas (10%), and freshwater lakes (15%). Close to the Skagerrak coast (~20 km) and at low altitude, the observatory experiences a maritime climate with relatively mild winters and moderately warm summers. The prevailing wind is westerly/south westerly. Figure S 1 shows ambient temperature and precipitation (2001–2018) at Birkenes. The nearest city is Kristiansand (population ~61 000) 25 km to the south/south-west.

2.2 Measurements and procedures

2.2.1 Off-line filter measurements

We collected OC/EC, organic tracers and PM mass filter samples using two low-volume samplers with a PM_{10} and a $PM_{2.5}$ inlet. Quartz fiber filters (Whatman QM-A; 47 mm in diameter) were pre-fired (850 °C; 3 h). We conditioned the filters [$20 \pm 1°C$; $50 \pm 5\%$ RH (relative humidity)] for 48 h before and after exposure and weighed them to obtain PM mass. We kept filters in petri slides and stored them at 4 °C after weighing and before OC/EC analysis. After OC/EC analysis and prior to organic tracer analysis the samples were stored at -18 °C. Two field blanks were assigned to each month of sampling and were treated in exactly the same manner regarding preparation, handling, transport and storage as the exposed filters, except that they were not inserted in the samplers. We collected one sample per sampler per week (168 hours), except for 14 August 2002–17 September 2008, when two samples were collected per sampler per week; at 24 h and 144 h intervals. The sampling inlets are 2 m above the Observatory roof, 5 m above the ground level (~226 m asl). The OC/EC and PM mass time series date back to February 2001 and organic tracers back to January 2008 (monosaccharide anhydrides) and January 2016 (sugars, sugar-alcohols and 2-methyltetrols).

We performed thermal-optical analysis (TOA, Sunset Laboratory OC/EC instrument), using transmission for charring correction. We used the Quartz temperature programme in 2001–2008 and EUSAAR-2 (Cavalli et al., 2010) from 2008. We compare the two temperature programmes for $PM_{2.5}$ samples collected in 2014 in Supplementary Sect. S1. OC/EC instrument performance is regularly inter-compared under the joint EMEP/ACTRIS quality assurance and quality control effort (e.g. Cavalli et al., 2013).

Until 2014, we determined monosaccharide anhydrides (levoglucosan, mannosan, galactosan) in PM_{10} using high-performance liquid chromatography high-resolution time-of-flight mass spectrometry (HPLC-HR-TOFMS) in negative electrospray ionization mode according to the method of Dye and Yttri (2005). After 2014, we use ultra-performance liquid chromatography (UPLC), with two Waters columns (2 x 2.1 x 150 mm HSS T3, 1.8 μm, Waters Inc.). Changing the column improved the chromatographic resolution, allowing the analysis of sugars, sugar-alcohols and 2-methyltetrols. We identified the monosaccharide anhydrides based on retention time and mass spectra (accurate mass and isotope pattern) of authentic standards (Table S 1). Isotope-labelled standards of levoglucosan, galactosan, arabitol, mannitol, trehalose and glucose were used as internal recovery standard (Table S 1).

Weekly OC/EC, PM_{10}, $PM_{2.5}$ are publicly available on EBAS (http://ebas.nilu.no). Mean values (daily/weekly/seaonal/annual) used below, merging of data from the old and new Birkenes sites, and quality assurance of the filter data are detailed in Sect. S1. We used the Mann-Kendall test (Mann, 1945; Kendall, 1975; Gilbert, 1987) to identify significant trends in the filter based measurements, and the

181   Theil-Sen slope (Theil, 1950; Sen, 1968; Gilbert, 1987) to quantify the trends (Sect. S2).

182

183   **2.2.2   Online measurement and source apportionment of absorption coefficients**

184   We determined Absorption coefficients (B_{Abs}) using a multi-wavelength absorption photometer (AE33

185   Aethalometer, Magee Scientific). Here we performed source apportionment using the aethalometer

186   model (Sandradewi et al., 2008) to determine eBC_{bb}/eBC_{ff}. However, the aethalometer model requires

187   *a-priori* knowledge of the aerosol Ångstrøm exponents (AAE), uncertainties which can lead to large

188   variation in the magnitude of the resulting time series and negative concentrations during some periods.

189   Often, the aethalometer model yields negative concentrations for any single input AAE pair. Therefore,

190   we also used a novel PMF application (Platt et al., in prep.) finding two factors, a low AAE factor (0.9)

191   and a higher AAE factor (2.04) identified as eBC_{ff} and eBC_{bb}, respectively. Uncertainties were assessed

192   using bootstrapping (n=2000). The advantages of the PMF are that no *a-priori* knowledge of the factor

193   AAEs is required, no periods of negative concentration result, deviations from a strict power-law

194   dependence of B_{Abs} on wavelength (e.g. due to degradation of light absorbing components in the

195   atmosphere or instrument errors/bias) are permitted, and poorly fitting data are assigned to a residual.

196   Meanwhile bootstrapping allows estimation of uncertainties, the methodology of the PMF analysis and

197   aethalometer data post-processing are detailed in Sect. S3 (Table S 2).

198

199   **2.3   FLEXPART model simulations**

200   We investigated the origin of the observed eBC with a Lagrangian transport model (FLEXPART v10.4,

201   Pisso et al., 2019). The model, powered by European Centre for Medium-Range Weather Forecasts with

202   137 vertical layers and a horizontal resolution of $0.1°×0.1°$ tracks simulated particles arriving at the

203   receptor 30 days backwards in time (retro-plume mode) and accounts for gravitational settling, dry and

204   wet deposition (Grythe et al., 2017), turbulence (Cassiani et al., 2014), unresolved mesoscale motions

205   (Stohl et al., 2005) and includes a deep convection scheme (Forster et al., 2007). Output consists of an

206   emission sensitivity ($0.5°×0.5°$ resolution), a quantitative measure for the particle mass concentration at

207   the receptor resulting from a unit emission flux at the Earth's surface. The emission sensitivity can also

208   be interpreted as a probability distribution field of the particle's origin, used in the present study to

209   identify possible source regions of eBC.

210

211   **2.4   Positive Matrix Factorization analysis on filter data**

212   We performed PMF ME2 (Canonaco et al., 2013) (See Sect. S3 for a description of the analysis principle

213   and S4 for its application to filter data) for samples collected in 2016-2018 (151 samples), using the

214   following as input data: OC (in $PM_{2.5}$ and $PM_{10-2.5}$), EC (in PM_{10}), levoglucosan, mannosan, galactosan,

215   arabitol, mannitol, trehalose, glucose, 2-methylerythritol, 2-methylthreitol, V, Mn, Ti, Fe, Co, Ni, Cu,

216   Zn, As, Cd, and Pb (all in PM_{10}), SO_4^{2}, NO_3^{-}, NH_4^{+}, Ca^{2+}, Mg^{2+}, K^+, Na^+, Cl^- (from open filter face).

217   Table S 3 shows miscellaneous settings of the PMF analysis of these data including missing data
218   treatment and an assessment of the PMF performance. The input data and error estimates were prepared
219   using the procedure suggested by Polissar et al. (1998) and Norris et al. (2014), see Sect. S3.

220   Source apportionment by PMF is based on the temporal variability of the components. It is
221   expected that significant contributions to carbonaceous aerosol at Birkenes is via long-range
222   atmospheric transport (LRT), alongside more local sources. Local and LRT sources will have different
223   temporal variability, and significant mixing of air masses and chemical transformation is expected for
224   the latter, i.e., factor profiles at Birkenes are expected to differ somewhat from emission profiles at the
225   source, even though the profile is distinctive enough for source attribution. Because of this we did not
226   attempt to constrain factor profiles via e.g. ME-2 (Canonaco et al., 2013) since Birkenes, as a relatively
227   clean rural background site, is unlikely to receive unprocessed emissions. Furthermore, mixed
228   contributions to a factor can in some cases be resolved *a posteriori* for source quantification (i.e. if it is
229   clear where mass should be reassigned), without potentially perturbing the output factor time series.

230   *Two previous studies have used factor analysis to study PM sources at Birkenes (Aamundsen et*
231   *al. (1992; Maenhaut, 2018). The present study focuses on carbonaceous aerosol, using OC, EC and*
232   *highly source specific organic tracers as input in addition to inorganic species and elements used by*
233   *Aamundsen et al. (1992) and Maenhaut (2018). This provides a different set of factors, based on*
234   *different input, hampering any reliable comparison of these studies.*

235

2.4.1   Identification of PMF factors

237   The biomass burning (BB) factor appears well confined in the PMF solution (Figure 2, Table S 4),
238   explaining all the monosaccharide anhydrides (95–98%). OC_{BB} was almost exclusively (87%) in the
239   fine fraction of PM_{10}. Other key qualifiers derived from the BB factor are the ratios listed in Table 1,
240   which are highly comparable to the results obtained by ^{14}C-analysis reported in the comprehensive
241   study by Zotter et al. (2014). The BB factor is elevated in the heating season and peaks in winter,
242   pointing to residential heating as the major source.

243   The TRA/IND factor explained most EC (50%), the majority of the trace elements Pb (84%), Zn
244   (82%), Cd (81%), As (78%), V (70%), Ni (69%), Cu (62%) and Co (42%) and a noticeable fraction of
245   SO_4^{2-} (20%), which suggests influence of various anthropogenic emissions. TRA/IND explained a
246   small fraction of fine OC (10%) and a negligible fraction of coarse OC (4%). The majority of OC
247   (88%) resides in the fine fraction, which is in line with its combustion-derived origin. The high EC
248   fraction unambiguously points to combustion processes, and the low OC/EC ratio (1.4 for $PM_{2.5}$)
249   towards a substantial, but not exclusive, influence from vehicular traffic. Cu and Zn result from brake
250   wear (Fomba et al., 2018), whereas tire wear is an additional source of Zn (Pacyna et al., 1986),
251   corroborating the influence of vehicular traffic to the TRA/IND factor. Ni and V are commonly
252   associated with combustion of heavy oil (Viana et al., 2008), As, Cd and Pb with combustion of coal,

253 and to a lesser extent oil, but also from metallurgic activity (Pacyna et al., 1986). The TRA/IND factor

254 has a minimum in summer and shows minor variability for the rest of the year. A similar drop in the

255 vehicular traffic factor in summer for Helsinki was shown by Saarikoski et al. (2008).

256 The PMF analysis confined the majority of coarse OC (53%) and essentially all (82–93%) of

257 the PBAP tracers (arabitol, mannitol, trehalose, and glucose) within one factor (PBAP). The PBAP

258 factor has a pronounced seasonal variability with increased levels in the vegetative season and nearly

259 absent outside of it, as previously described for coarse OC (Yttri et al., 2007a) and PBAP tracers (Yttri

260 et al., 2007b) at Birkenes.

261 2-methyltetrols (92–96%) are oxidation products of isoprene (Claeys et al., 2004) and are almost

262 exclusively attributed to the BSOA$_{SRT}$ (SRT=Short Range Transport) factor, which explains 9% of fine

263 OC and 13% of coarse OC. The complete absence of EC and the presence of SO$_4^{2-}$ (17%) underpins the

264 secondary nature of this factor, which is present in summer with tail ends in late spring an early fall. The

265 BSOA$_{SRT}$ time series increases abruptly in the transition May/June, as leaves unfold, and subsides

266 equally rapid in the beginning of October when trees shed their leaves. The near absence of 2-

267 methyltetrols prior to May/June suggests that the 0.5–1.5 months earlier onset of the vegetative season

268 in Continental Europe (Rötzer and Chmielewski, 2001) is not reflected by the 2-methyltetrols

269 observations at Birkenes, indicating a short atmospheric lifetime for 2-methyltetrols. Consequently,

270 local isoprene emissions likely explain the observed concentrations of 2-methyltetrols at Birkenes,

271 questioning to what extent the BSOA$_{SRT}$ factor includes a continental BSOA contribution. Similar

272 sources (deciduous and coniferous trees), temperature dependent emissions, and formation rates, suggest

273 that particulate phase oxidation products of mono- and sesquiterpenes are accounted for by the isoprene-

274 derived BSOA$_{SRT}$-factor as well, but with a similar issue concerning local versus LRT contribution, as

275 proposed for the 2-methyltetrols.

276 The MIN factor is defined by its content of Ti (93% of total), Fe (75%), Mn (52%) and Ca^{2+}

277 (39%) (Figure 2, Table S 4), well-known constituents of mineral dust (e.g. Alastuey et al., 2016). It

278 also contains some of the elements that dominate the TRA/IND factor, including Co (43%), Cu (20%),

279 Ni (17%) and V (14%), indicating anthropogenic influence. Notably, 31% of fine OC is attributed to

280 the MIN factor, whereas it explains 13% of coarse OC. This corresponds to that reported by Kyllönen

281 et al. (2020) for the Subarctic site Pallas (Finland) where 29% of the fine OC was apportioned to the

282 mineral dust factor. Waked et al. (2014) found a similar result for Lens (France) where the mineral

283 dust factor explained 15% of OC. No information on the size distribution was available in Kyllönen et

284 al. (2020) and Waked et al. (2014), whereas in the present study 86% of OC in the MIN factor resides

285 in the fine fraction of PM$_{10}$. Since mineral dust typically resides in the coarse fraction of PM$_{10}$ (Ripoll

286 et al., 2015), one would expect the same for its carbon content, e.g. as CaCO$_3$. More efficient

287 deposition of coarse mode mineral dust during LRT is one possible explanation but mixing of air

288 masses is more likely, as 13% of the EC also resides in this factor. The high OC/EC ratio in the

289   unweighted MIN factor profile (18 for $PM_{2.5}$) indicates a minor primary combustion particle influence,

290   and the absence of levoglucosan shows that the EC content originates from fossil fuel combustion

291   (consistent with some TRA/IND influence). Using Eq. (1), 8% of the MIN factor's fine OC content is

292   attributed to combustion of fossil fuel OC (OC_{PrimFF}), whereas the corresponding percentage for PM_{10}

293   OC is 7%. If all Ca^{2+} and Mg^{2+} in the MIN factor was present as either Calcite ($CaCO_3$) or Dolomite

294    $CaMg(CO_3)_2$, the CO_3^{2-}-carbon would account for no more than 3% of the factor's PM_{10} OC content,

295   and 22% if all reside in its coarse fraction. This shows that the OC content of the MIN factor mostly

296   originates from other sources than mineral dust and combustion of fossil fuel. The MIN factor is most

297   abundant in spring and early summer, as seen by Waked et al. (2014), and is associated with southern

298   air masses, as seen for the dry and warm period in the transition of May/June 2018 (Figure 3) when

299   there was a pronounced peak in the MIN factor time series (Figure 2). Indeed, the mean ambient

300   temperature was 4˚C higher in May 2018 than for May 2001–2018, whereas it was 2.4˚C higher for

301   June 2018 than for June 2001–2018. We thus suggest that the climatological conditions that activate

302   mineral dust sources also favour BSOA formation and that the majority of both fine (92%) and coarse

303   fraction (78%) OC in the MIN factor is LRT BSOA ($OC_{BSOA,LRT}$).

304

305    $$OC_{Fossil,primary,MIN} = [EC_{MIN}] \; x \left(\frac{OC}{EC}\right)_{TRA/IND}, \left(\frac{OC}{EC}\right)_{TRA/IND} = 1.4 \qquad\qquad Eq. 1$$

306

307   The majority of NH_4^+ (77%) and NO_3^- (68%) reside in the NH_4NO_3 factor, which points to

308   secondary inorganic aerosol (SIA) formation during LRT. This is supported by a noticeable contribution

309   of SO_4^{2-} (35%) to the NH_4NO_3 factor, as well. The factors content of NO_2 (30%) points towards a

310   combustion-derived origin of NO_3, as does EC (13%). The factor's OC content is comparable to that

311   seen for the BB factor. The factor is most pronounced in winter and spring.

312   The sea salt (SS) aerosol factor was recognized by its high Cl^- (96%), Na^+ (87%) and Mg^{2+} (79%)

313   fractions. The K^+/Na^+ (0.036), Ca^{2+}/Na^+ (0.034) and SO_4^{2-}/Na^+ (0.282) ratios derived from the SS factor

314   closely resemble these ratios in sea water (0.037, 0.038 and 0.252) (Stumm and Morgan, 1996), further

315   demonstrating the successful separation of this factor.

316

317   **3.   Results and discussion**

318   **3.1   Levels and trends of carbonaceous aerosol and organic tracers**

319   Annual mean carbonaceous aerosol concentrations at Birkenes (2001–2018) are among the lowest in

320   Europe (Yttri et al., 2007a; Yttri et al., 2019), with OC from 0.56–1.07 µg C m^{-3} for PM_{10} and 0.50–

321   0.93 µg C m^{-3} for $PM_{2.5}$, and EC from 0.05–0.15 µg C m^{-3} (Figure 4; Table S 4). EC, being from

322   combustion that generates fine PM, was almost exclusively associated with $PM_{2.5}$, whereas OC was

323   abundant also in the coarse fraction ($PM_{10-2.5}$), particularly in summer and fall (Figure 4). The

324   correlation between OC and EC varied by season (Table S 6) and was highest in the heating season,

9

325 reflecting the contribution of biogenic, non-EC sources, such as BSOA and PBAP in the vegetative

326 season. The higher R^2-values for $PM_{2.5}$ compared to PM_{10} can partly be attributed to PBAP, which

327 mainly resides in $PM_{10-2.5}$.

328   The variability of the annual mean OC (15–22%) and EC (27%) concentrations was comparable

329 to the major secondary inorganic aerosol (SIA) (SO_4^{2-}, NO_3^-, NH_4^+) and sea salt (SS) aerosol species

330 (Na^+, Mg^{2+}, Cl^-) (25–31%). A difference of $> 60\%$ between consecutive years was observed for OC and

331 EC in PM_{10} and $PM_{2.5}$, whereas 160% was seen for OC in $PM_{10-2.5}$. It is important to note that despite

332 decades of SO_2, NH_3 and NO_x mitigation efforts, SIA dominates PM_{10} mass (29–52%) most years,

333 followed by carbonaceous aerosol (24–40%) and SS aerosol (10–28%) (Figure 5; Table S 7). SIA

334 constituents were also the largest PM_{10} fraction during air pollution episodes (Table S 8), reflecting that

335 Birkenes is affected by major SIA precursor emission regions in Continental Europe.

336   Levels of total carbon (TC) and PM fractions are shown in Table S 9 and Table S 10, respectively

337 for completeness. In the following sections we discuss the OC and EC fractions separately in detail.

338

3.1.1 Organic carbon

340 We found no significant trend for OC in PM_{10} (OC_{PM10}). For fine OC in $PM_{2.5}$ ($OC_{PM2.5}$) there was a

341 minor decrease (-0.8% yr^{-1}), whereas there was a minor increase for coarse OC ($OC_{PM10-2.5}$) (0.8% yr^{-1})

342 (Table S 11). The anthropogenic fraction of OC observed at Birkenes likely has a downward trend as

343 found for EC (Sect. 3.1.2), but the substantial influence of natural sources demonstrated in the present,

344 as well as in previous, studies (Yttri et al., 2011b), explains the general lack of trends for OC.

345   The OC time series are characterized by two years where the annual mean was substantially

346 higher (2006) and lower (2012) than the proceeding and the following year (Figure 4). The increased

347 level in 2006 was most pronounced in the fine fraction and in all seasons except spring, whereas the

348 drop in 2012 mainly was attributed to the coarse fraction and was observed in all seasons. The $OC_{PM10-2.5}$

349 annual mean time series is characterised by a stepwise increase from 2001 up to, and including, 2006,

350 after which the concentration dropped and showed minor annual variability, except for the very low

351 annual mean of 2012. After 2015, there are indications of a similar stepwise increase as seen for 2001–

352 2006.

353 The $OC_{PM10-2.5}$ contribution to OC_{PM10} ranged from 18–35% on an annual basis (2001 excluded due to

354 data capture <50%), and levels were highest in summer and fall. Previous studies (Simpson et al.,

355 2007; Yttri et al., 2011a,b) showed that BSOA largely dominates the fine carbonaceous aerosol in

356 summer at Birkenes, whereas the present study shows that Birkenes regularly experiences major air

357 pollution events in spring, as a result of LRT (Table S 4, Table S 7 and Table S 8). Hence, both

358 biogenic sources and LRT explain the observed seasonality of fine OC.

359   We attribute elevated $OC_{PM2.5}$ in winter 2010 to residential wood burning emissions as discussed

360 in Sect. 3.2.1. Only on five occasions did the seasonal mean of $OC_{PM2.5}$ exceed 1 µg C m^{-3}, four of those

in the first three years of the time series. The highest mean was observed in summer 2002 (1.4 µg C m^{-3}) when wildfires in Eastern Europe influenced Birkenes (Yttri et al., 2007a). The four other occasions, spring (2001, 2002, 2003 and 2018), also saw prolonged episodes of PM air pollution with the hallmark of LRT; i.e., elevated SO_4^{2-}, NO_3^- and NH_4^+. According to our PMF analysis (See Sect. 3.2) there are several anthropogenic and biogenic sources likely to contribute to fine OC at Birkenes, whereas coarse fraction OC is dominated by a single source, PBAP (Yttri et al., 2007 a,b; Yttri et al., 2011 a,b; Glasius et al., 2018). Hence, it is not surprising that $OC_{PM2.5}$ was the dominant OC fraction, accounting for 70–89% OC_{PM10} on an annual basis.

3.1.2   Elemental carbon

Notably, EC levels dropped from 2007–2008, contrasting with the annual mean OC time series, (Figure 4 and Table S 5). This major downward trend of EC clearly points to changing source contributions to EC at Birkenes. We rarely observed seasonal means exceeding 0.15 µg C m^{-3}; only in winter 2006, 2007 and 2010, spring 2001, 2003 and 2007, and fall 2005 and 2011. Weekly samples exceeded 0.5 µg C m^{-3} for three samples only, all associated with LRT.

A statistically significant reduction was calculated for EC in PM_{10} (-3.9% yr^{-1}) and $PM_{2.5}$ (-4.2% yr^{-1}) (Table S 11), corresponding well with SO_4^{2-} (-3.8% yr^{-1}) and $PM_{2.5}$ (-4.0% yr^{-1}). The trend for EC was most pronounced in spring and summer (-4.0 – -5.9% yr^{-1}) (Table S 12), as seen for SO_4^{2-} (-4.2 – -6.4% yr^{-1}) and $PM_{2.5}$ (-3.0 – -4.4% yr^{-1}) (Table S 12). The EMEP model finds a somewhat lower reduction for EC (-3.0 % yr^{-1}) for 2001–2017 (EEA, 2020) with the largest emission reductions for the road transport (83 kt; -3.6% yr^{-1}) and off-road categories (44 kt; -3.7 % yr^{-1}) (https://www.ceip.at), which are sectors with a minor seasonal variability. We suggest that these sectors explain the downward trend observed for EC at Birkenes, and that the seasonality of the EC trend is due to the substantial contribution from less abated sources, such as domestic heating in winter and fall. Notably, modelled EC emissions are unchanged for the category other stationary combustion for 2001–2016 (-1 kt; -0.08% yr^{-1}) (https://www.ceip.at), which includes residential heating, and wood burning in particular.

Effective abatement of SIA precursors and fossil EC, along with a high natural source contribution to OC, largely explains why the OC fraction increased significantly for $PM_{2.5}$ (+3.2% yr^{-1}) and PM_{10} (+2.4% yr^{-1}), whereas it decreased for the EC fraction (-3.9 – -4.5% yr^{-1}) (Table S 13). The largest increase (OC) and decrease (EC) was seen in the vegetative season (Table S 14) when BSOA and PBAP increase and the influence of poorly abated sources such as domestic heating is low. Consequently, these results demonstrate a long-term change in the aerosol chemical composition at Birkenes and thus also in the relative source composition of PM.

3.1.3   Levoglucosan

Levels of levoglucosan and other organic tracers are given in Table S 15, whereas other organic tracers

11

397 (arabitol, mannitol, trehalose, glucose, and 2-methyltetrols) are discussed in Sect. S6.

398   The statistically significant decrease of levoglucosan (-2.8% yr^{-1}) at Birkenes for 2008–2018

399 (Figure 6; Table S 11), and the fact that biomass burning levels observed at Birkenes are largely

400 explained by continental emissions (Figure 7) might indicate that wood burning emissions in continental

401 Europe are declining. However, surprisingly, we find no significant trend for levoglucosan on a seasonal

402 basis (Table S 12). Furthermore, and although one should be careful drawing conclusions from non-

403 significant outcomes, it is worth noting that the levoglucosan to EC ratio most likely increased (+2.8%

404 yr^{-1} (PM$_{10}$), CI (Confidence Interval) = -3.5 – +6.5% yr^{-1} and +2.3% yr^{-1} (PM$_{2.5}$), CI = -2.2 – 5.0 % yr^{-1})

405 for the period 2008–2018, whereas it most likely decreased (-1.8% yr^{-1} (PM$_{10}$), CI = -10.6 – +1.8 and -

406 3.6% yr^{-1} (PM$_{2.5}$), CI = -9.8 – +1.3% yr^{-1}) for the levoglucosan to OC ratio (Table S 13). A more

407 efficient abatement of fossil sources than biomass burning would explain the levoglucosan to EC

408 increase, whereas we fail to see a similar trend for the levoglucosan to OC ratio, as prevailing natural

409 sources mask the assumed reduction in fossil OC of anthropogenic origin.

410   The levoglucosan time-series provides a hitherto unprecedented opportunity to validate European

411 residential wood burning emission inventories at a decadal time basis. Unfortunately, the inventories

412 suffer from non-harmonized emission reporting and lack of condensable organics (van der Gon et al.,

413 2015, Simpson et al., 2019), which hampers any reliable attempt for such validation. Given the

414 uncertainties in the trend calculations (i.e. annual vs. seasonal trends), more work is needed to

415 investigate trends in levoglucosan and biomass burning, foremost by continuation of the actual time

416 series. Such efforts should be initiated immediately given the numerous studies that point to residential

417 wood burning as a major source of air pollution in Europe (e.g. Denier van der Gon et al., 2015; Yttri et

418 al., 2019).

419

420 **3.2   Sources of carbonaceous aerosol at Birkenes**

421 We used PMF to apportion carbonaceous aerosol at Birkenes for 2016–2018. The time period was

422 restricted by organic tracer data availability. Carbonaceous aerosol annual means for 2016–2018 were

423 within the long-term annual mean (±SD) for OC, and only slightly lower for EC in 2016 and 2017 and

424 are thus representative of the longer time series. Six out of seven factors identified in contribution-

425 weighted relative profiles from PMF (Figure 2; Table S 4) were associated with significant amounts of

426 carbonaceous aerosol. This includes factors for mineral dust-dominated (MIN), which OC content is

427 associated mainly with LRT BSOA (BSOA$_{LRT}$), traffic/industrial-like (TRA/IND), biogenic secondary

428 organic aerosol (BSOA$_{SRT}$), which is short-range transported, primary biological aerosol particles

429 (PBAP), biomass burning (BB), and ammonium nitrate dominated (NH$_4$NO$_3$). The sea salt aerosol

430 factor (SS) had a negligible (<1%) carbonaceous aerosol content.

431   The MIN factor (31%) explained the largest fraction of fine OC, whereas BB (17%), NH$_4$NO$_3$

432 (17%) and PBAP (16%) had almost equally large shares, as did TRA/IND (10%) and BSOA$_{SRT}$ (9%)

433 (Figure 8). Coarse OC was by far most abundant in the PBAP factor (53%), whereas $BSOA_{SRT}$ (13%),

434 MIN (13%) and NH_4NO_3 (12%) explained almost equally large shares. For the other factors, coarse OC

435 was minor. EC was apportioned to only five factors of which TRA/IND (50%) dominated by far. BB

436 made a 21% contribution and MIN and NH_4NO_3 equally large shares (13%). The 3% apportioned to

437 PBAP is an assumed analytical artefact (See Sect. 3.2.2 for details).

438   The BB, NH_4NO_3 and TRA/IND factors are considered entirely anthropogenic, $BSOA_{SRT}$ and

439 PBAP exclusively natural, whereas MIN is mixed (Figure 8). Natural (54%) and anthropogenic (46%)

440 sources contributed almost equally to fine OC (Figure 8) annually, so also in spring and fall (51%

441 natural), whereas natural sources prevailed in summer (77%) and anthropogenic in winter (78%).

442 Natural sources dominated coarse OC annually (78%) and in all seasons (70–91%), except winter (37%).

443 We consider the minor fraction of coarse OC attributed to carbonate-carbon (3%) to be of natural origin.

444 The findings for OC in PM_{10} are rather like that of $PM_{2.5}$, only that the natural contribution is somewhat

445 more pronounced due to the influence from a mostly naturally influenced coarse OC fraction.

446

3.2.1   Anthropogenic carbonaceous aerosol sources

448 According to PMF, BB accounted for 14–17% of OC annually, considering both $PM_{2.5}$ and PM_{10} vs.

449 only 6% of coarse OC. BB was by far the major contributor to OC in winter (35–37%) and by far the

450 most minor contributor in summer (2–3%) (not considering SS). Spring and fall are transition seasons

451 where BB still made a substantial 14–19% contribution to OC. BB explained 22% of EC annually

452 (excluding EC_{PBAP}, which we assume is an analytical artefact, see Sect. 3.2.2), hence fossil fuel

453 combustion (78%) was the major source. Emissions from residential wood burning increased in the

454 heating season but fossil fuel sources dominated EC even in winter (66%). It cannot be excluded that

455 part of levoglucosan originates from wildfires in summer, spring, and fall, though this itself may be due

456 to anthropogenic activity. However, the levoglucosan/mannosan (L/M) ratio indicates minor variability

457 in the source composition throughout the year (See Sect. S5), suggesting one dominating source.

458 The 78%:22% split of EC into fossil fuel combustion and biomass burning derived from PMF is

459 supported by high time resolved concentrations of eBC_{BB} and eBC_{FF} derived from multiwavelength

460 aethalometer measurements of the absorption coefficient, following the PMF-approach of Platt et al.

461 (in prep.). With this approach we find $eBC_{BB}/eBC_{TOT}=28\%$ (Table 2). Meanwhile, using the

462 aethalometer model and $AAE_{FF}=0.9$ and $AAE_{BB}=1.68$ (Zotter et al. 2017) as input we find

463 $eBC_{BB}/eBC_{TOT}=48\%$, however the aethalometer model is extremely sensitive to the input AAE and the

464 AAE values suggested by Zotter et al. (2017) are only recommended where no *a priori* information on

465 the AAEs is available and a significant advantage of the PMF approach by Platt et al. (in prep.) is that

466 the AAE is an output.

467   Source regions of elevated (70th percentile) and low (30th) winter and summertime eBC_{BB} (and

468 eBC_{FF}) observed at Birkenes for 2018 were studied using the approach of Hirdman et al. (2010). The

469 results show that Birkenes is a receptor of LRT exclusively from Continental Europe for elevated eBC_{BB}
470 and eBC_{FF} levels (Figure 7), both in summer and winter. This is consistent with a lack of diurnal
471 variation in either eBC_{BB} or eBC_{FF}, likely because there are few local sources at Birkenes. The main
472 source regions extend from the Atlantic coast in the west to the Ural Mountains in winter, whereas the
473 regions in summer are confined to Eastern Europe and western Russia (but not as far east as the Urals).
474 Notably, the Nordic countries do not contribute to elevated levels except for southern parts of Finland
475 in summer. The footprints are almost identical for eBC_{BB} and eBC_{FF} both for summer and winter. High
476 similarity in winter is not a surprise, as the footprint covers such a wide area and because wood burning
477 for residential heating is common in several European countries. The summertime footprint is a
478 subsection of the wintertime footprint that covers an area well-known for severe wildfires and
479 agricultural fires (Stohl et al., 2007 and Yttri et al., 2007a), and thus agrees with previous studies.
480 Further, Sciare et al. (2008) point to the European countries bordering the Black Sea as having high
481 carbonaceous aerosol of fossil origin. Low eBC_{BB} and eBC_{FF} levels at Birkenes are consistent with air
482 masses that have an oceanic or terrestrial origin at high latitudes, mainly from the Arctic. Notably, the
483 30% highest values explain 74% of eBC_{BB} at Birkenes for the actual period, hence LRT is decisive not
484 only for episodes of high concentrations but also largely explains the mean concentration. All eBC_{BB}
485 and eBC_{FF} observations included in the 70th percentile was made in winter despite the less pronounced
486 seasonality of eBC_{FF} compared to eBC_{BB}.

487 To generate a longer BB time series of OC_{BB} and EC_{BB} we combine the levoglucosan time series
488 (2008–2018) with levoglucosan/OC and levoglucosan/EC ratios derived from the BB factor of the PMF
489 analysis (Table 1; See Sect. S 5 for details). Depletion of levoglucosan by OH oxidation is more likely
490 in summer (Hoffmann et al., 2010; Yttri et al., 2014), still we assume that levels mostly reflect biomass
491 burning emissions in all seasons.

492 EC_{BB} levels were elevated in the heating season (Figure 9; Table S 16). A strong temperature
493 influence is illustrated by a 9°C difference in the 25th percentile of wintertime temperatures in 2015 (-
494 0.3°C) and 2010 (-9.3°C) (Figure S 1), which experienced the lowest (19 ng m^{-3}) and the highest (84 ng
495 m^{-3}) winter-time mean concentration of EC_{BB}, respectively. Winter 2010 was exceptionally cold due to
496 a negative North Atlantic Oscillation, and the only occasion when EC_{BB} exceeded EC_{FF}, with annual
497 mean EC_{BB}>60% higher than the long-term mean. Pronounced interannual variability was seen for the
498 wood burning contribution in winter, from 21–60% to EC, with the lowest fractions occasionally
499 matched by those in spring and fall, typically ranging between 20–30%. EC_{BB}/EC was small in summer
500 (4–15%), considerably less than other seasons, except in 2008, where we calculate a substantial 30–40%
501 contribution. Levoglucosan cannot be used to differentiate emissions from residential wood burning,
502 wildfires and agricultural fires; exceptions are major wildfire and agricultural fire episodes identifiable
503 by unusual high concentrations and traced by source receptor models/satellite data for plumes/burnt
504 areas (Yttri et al., 2007a, Stohl et al., 2007). Influence from major wildfires in Eastern Europe caused a

14

505 summertime peak in fine OC and EC in 2002 at Birkenes (Yttri et al., 2007a). In June 2008, the largest
506 wildfire in Norway since the Second World War raged 25 km northeast of the Birkenes Observatory,
507 with an area of 30 km^2 burnt. The observatory was downwind of the fire on only one day, according to
508 FLEXPART (Figure S 2). Despite this, the levoglucosan concentration for the weekly filter sample was
509 153 ng m^{-3}, by far the highest in one decade of sampling. Notably, the annual mean concentration of
510 levoglucosan for 2008 increased by nearly 35% and EC_{bb} contributed significantly to EC for summer
511 2008.

512 The seasonality of OC_{BB} (Figure 9) was like EC_{bb}. Mean wintertime OC_{BB}/OC was 39–40% and
513 >50% in 2010 and 2012, considering both PM_{10} and $PM_{2.5}$. The summertime contribution was typically
514 <5%, reflecting both low levoglucosan levels and major influences from BSOA and PBAP, which peak
515 in summer. Notably, five of the seven highest weekly OC concentrations for the PM_{10} time-series were
516 attributed to emissions from major wildfires in Eastern Europe, i.e., August 2002, and May/September
517 2006, and thus prior to the initiation of the levoglucosan time series. The local wildfire episode in
518 summer 2008 caused a substantial increase in OC_{bb}/OC (13–18%), which is within the lower range of
519 that observed for spring (12–27%) and fall (13–39%).

520

521 **3.2.2 Biogenic carbonaceous aerosol sources**
522 The general lack of PBAP tracers in the MIN (<1%) and SS (<2%) factors and no sea salt and Ti in the
523 PBAP factor, implies that soil and sea spray aerosol do not contribute to PBAP at Birkenes, although
524 this has been shown elsewhere (O'Dowd et al., 2004; Jia and Fraser, 2011). PBAP represented by
525 glucose, arabitol and mannitol appears to be associated with leaves rather than soil material and to be a
526 source of local origin (Samaké et al., 2019). However, even large PBAP, such as birch pollen (avg. diam.
527 22 μm), has a potential for long range atmospheric transport of 1000 km due to its low density,
528 hydrophobic nature, release during favourable dispersion conditions, and (often) emission height > 10
529 m (e.g. Sofiev et al., 2006; Skjøth et al., 2007).

530 The PBAP factor concentration was nearly one order of magnitude higher in summer and fall
531 than in winter and was the major contributor to coarse OC for all seasons except winter, particularly in
532 summer (54%) and fall (69%) (Figure 8). These are conservative estimates, as 3–9% of the PBAP tracers
533 reside in the $BSOA_{SRT}$ factor, likely due to co-variability, as there is no scientific evidence linking
534 biologically formed sugars and sugar-alcohols to abiotic formation of BSOA. Notably, the PBAP factor
535 explained 20–26% of fine OC in summer and fall, being the major contributor in fall. Consequently,
536 PBAP was the major contributor to OC even in PM_{10} in summer (31%) and fall (40%). The PBAP factor
537 even explained 16% of fine OC (Figure 8) annually, corresponding to 0.084 μg C m^{-3}, which is
538 marginally lower than the factor's content of coarse OC (0.113 μg C m^{-3}). Combined, this made PBAP
539 the most abundant contributor to OC in PM_{10} along with the MIN factor (both 26%). Some PBAP tracers
540 partly reside in the fine mode (Carvalho et al., 2003; Yttri et al., 2007b) but the 43% OC_{PBAP} found in

the fine fraction in the present study is higher than what has previously been reported for the actual PBAP tracers at Birkenes; i.e. 6–7% (arabitol and mannitol), 20% (trehalose), and 33% (glucose) (Yttri et al., 2007b). It cannot be excluded that the PBAP factor contains some fine OC from other sources e.g. due to condensation, but although there is a seasonal co-variability with the $BSOA_{SRT}$ factor, only 2–3% of the 2-methyltetrols were explained by the PBAP factor and there was a low correlation between the PBAP and the $BSOA_{SRT}$, which questions this hypothesis.

Arabitol and mannitol are well-known tracers of fungal spores (Bauer et al., 2008), one of the most abundant sources of PBAP (Elbert et al., 2007). Applying an OC to mannitol ratio of 5.2–10.8 for fungal spores (Bauer et al., 2008; Yttri et al., 2011a), we estimate that 11–22% of OC_{PBAP} (in PM_{10}) comes from this source. Glucose is one of the primary molecular energy sources for plants and animals, a building block of natural dimers and polymers (e.g. sucrose and cellulose), and thus ubiquitous in nature and considered a PBAP tracer of general character, and clearly important for allocation of carbon mass to PBAP. Nevertheless, a wider range of organic tracers ought to be tested in future PMF studies to explore the potential of further separation of the highly heterogenic PBAP source, including cellulose, but also amino acids. A greater diversity of PBAP tracers may also provide a more correct PBAP estimate. The PMF approach used in the present study gives a somewhat higher, but overlapping, estimate of OC_{PBAP} at Birkenes for August 2016–2018 than Latin Hypercube sampling (LHS) for August 2009 (Yttri et al., 2011b) (Table 3). The LHS approach was based on *a priori* emission ratios, with uncertainty ranges estimated in a similar way to a Monte Carlo analysis (though less computationally extensive), and considered only the sum of fungal spores and plant debris as OC_{PBAP}, based on mannitol (fungal spores) and cellulose (plant debris), whereas the PMF approach may pick other contributing, i.e. co-varying, sources.

The 3% EC in the PBAP factor is substantially less than the 16% reported by Waked et al. (2014), which stated that atmospheric mixing, PMF limitations and artifacts caused by thermal-optical analysis could be plausible explanations. In the present study, low levels of coarse fraction EC occasionally appear in summer and fall (Table S 5), following the seasonality of PBAP. This finding does not exclude any of the three possibilities proposed by Waked et al., (2014), but supports the suggestion by Dusek et al. (2017) that PBAP, or at least some types of PBAP, chars and evolves as modern carbon EC during thermal-optical analysis. If EC_{PBAP} indeed is an analytical artefact, then constraining the PBAP factor to contain no EC, as suggested by Weber et al. (2019), should be done with caution, as it will wrongfully apportion pyrolytic carbon generated from PBAP as EC to another source. Thus, EC_{PBAP} should rather be interpreted as OC_{PBAP}. With no EC_{SS}, no $EC_{BSOA,SRT}$ and EC_{PBAP} an assumed analytical artefact, EC can be apportioned into a fossil fuel category (EC_{FF}), consisting of the MIN, TRA/IND, and NH_4NO_3 factors (explains 0.2% of levoglucosan), and a non-fossil biomass burning category (EC_{BB}), the BB factor. Some EC has been reported from meat cooking (Rogge et al., 1991), which is a non-fossil source, but its influence is minor at Birkenes, as it has not been observed

577 based on concurrent ACSM-measurements and is not accounted for by levoglucosan.

578 Our PMF results support the use of $OC_{PM10-2.5}$ as a proxy of OC_{PBAP}, which has a pronounced

579 seasonality (Figure 4) with the highest seasonal mean concentration observed in summer for 15 of the

580 studied years and in fall for the three others (Table S 5). The seasonal mean exceeded 0.5 µg C m^{-3} on

581 two occasions only; fall 2005 and fall 2006. With a few exceptions, $OC_{PM10-2.5}$ contributed more than

582 30% to OC_{PM10} in summer and fall. The highest relative contribution (45–50%) to OC_{PM10} were

583 exclusively observed in fall (2004, 2005, 2006, 2008, 2014, 2017), likely reflecting a combination of

584 high $OC_{PM10-2.5}$ concentrations and fine fraction OC_{BSOA} declining at this time of the year. $OC_{PM10-2.5}$

585 made a substantially lower contribution to OC_{PM10} in winter (mean: 13%) and in spring (mean: 19%)

586 compared to summer and fall, although contributions exceeding 25% were observed in spring for certain

587 years. Notably however, the PBAP factor explains 16% of fine OC, which would not be accounted for

588 using coarse OC as a proxy of OC_{PBAP}.

589 These numbers suggest that PBAP is a major, continuous contributor to OC in PM_{10} at Birkenes

590 for a period of nearly two decades, and that it largely explains the seasonality. Estimates of PBAP levels

591 in the continental European rural background environment are largely lacking and should be undertaken

592 to explore PBAPs potential importance. With a longer vegetative season and a different climate, the

593 PBAP flux might be larger in more southerly countries, although the relative contribution might be lower

594 due higher overall OC levels. Waked et al. (2014) found that OC_{PBAP} accounted for 17% of OC in PM_{10}

595 on an annual basis for an urban background site in Lens (Northern France), and between 5–6% in

596 winter/spring and 27–37% in summer/fall using PMF for source apportionment. These fractions are

597 comparable to those observed in the present study, albeit concentrations calculated by Waked et al.

598 (2014) were higher.

599 PBAP is a large OC source not included in many models. OC model closure, both for overall

600 levels and seasonality, would thus likely be improved in many cases by its inclusion. This appears to be

601 particularly important for regions with low anthropogenic influence. Birkenes is situated in the Boreo-

602 nemorale zone, a transition zone of the Nemorale and the Boreal zone, hence, findings made for this site

603 likely gives an indication of what can be expected for this scarcely populated, circumpolar region, which

604 by far is the largest terrestrial biome of the Northern Hemisphere. Hence, measurements in unperturbed

605 areas should include PBAP for a better understanding of background conditions. In turn, such

606 measurements may improve e.g. climate models; i.e., the aerosol climate effect under relatively clean

607 conditions.

608 Modelled estimates suggest a 10–40% contribution of BSOA to fine OC annually at Birkenes

609 (Simpson et al., 2007; Bergström et al., 2012). Hence, the 9% contribution of $OC_{BSOA,SRT}$ to fine OC,

610 and the 13% contribution to coarse OC (10% to OC in PM_{10}) found in the present study by PMF, appears

611 to be in the lower range. Further, 3–9% of the PBAP tracers reside in the $BSOA_{SRT}$ factor, hence some

612 of its OC content may rather be attributed to PBAP, further lowering the OC content of the $BSOA_{SRT}$

17

factor but strengthening coarse OC as a proxy of PBAP. $BSOA_{SRT}$ made a negligible contribution to fine, coarse and PM_{10} OC in all seasons, except in summer (22–25%), apparently contradicting previous studies that unambiguously point to BSOA as the major carbonaceous aerosol source at Birkenes in the vegetative season (Simpson et al., 2007; Yttri et al., 2011b). Note that a prevailing BSOA source in summer is considered a normal situation also for European rural background environment in general (e.g. Gelenscer et al., 2007), not only for Birkenes. Table 3 shows that $OC_{BSOA,SRT}$ obtained by PMF for August 2016–2018 is substantially lower than that obtained by LHS for August 2009 (Yttri et al., 2011b). Although not obtained for the same year, we argue that methodology rather than climatology explains most of the difference. $OC_{BSOA,LHS}$ provides an upper estimate including all modern carbon, local and from LRT (excluding biomass burning and PBAP fungal spores and plant debris), whereas $OC_{BSOA,SRT}$ gives a lower estimate accounting for locally formed BSOA.

It is less likely that anthropogenic secondary organic aerosol (ASOA) resides in the $BSOA_{SRT}$-factor, as ASOA precursors result from combustion processes and evaporative losses. Further, Yttri et al. (2011a) found higher ASOA concentrations in the Norwegian rural background environment in winter compared to summer, which is opposite of $BSOA_{SRT}$, hence co-variation and/or apportionment to the same factor do not appear likely. ASOA is less abundant than BSOA at Birkenes, as calculated by Simpson et al. (2007) and Bergström et al. (2012), but the estimates vary substantially and are very uncertain (Spracklen et al., 2011), particularly for ASOA (from 1% to 10–20%). It is difficult to predict which PMF factor(s) accounted for ASOA, but for the sake of separating OC into a natural and an anthropogenic fraction we assume that ASOA is not part of neither $BSOA_{SRT}$ nor the PBAP factor, which we consider as exclusively natural factors. To provide an upper estimate of the natural sources (Figure 8), we neither consider it part of the MIN factor.

With 90% (in PM_{10}) and 92% (in $PM_{2.5}$) of the MIN factor's OC content attributed to LRT BSOA ($OC_{BSOA,LRT}$) (See Sect. 2.4.1), the combined contribution of locally formed BSOA ($OC_{BSOA,SRT}$) and $OC_{BSOA,LRT}$ to OC in PM_{10} and $PM_{2.5}$ would be 34–38% on an annual basis, 37–41% in spring and 50–57% in summer. From this we can deduct that 1/3 of BSOA is of local origin, whereas 2/3 are long-range transported. For August 2016–2018, the joint contribution of $OC_{BSOA,SRT}$ and $OC_{BSOA,LRT}$ to OC in PM_{10} is 31%, corresponding better with the LHS estimate (Table 3) but still noticeably lower. Notably, $OC_{BSOA,SRT}$, $OC_{BSOA,LRT}$ and OC_{PBAP} combined contributed 79% to OC in PM_{10} in August 2016–2018, which exactly matches the sum of $OC_{BSOA,LHS}$ and $OC_{PBAP,LHS}$ to OC in PM_{10} in August 2009. This suggests that LHS and PMF apportion an equally large amount of OC to natural sources but that the split between BSOA and PBAP likely differs. It is evident that the LHS-approach provides an upper estimate of BSOA (Gelenscer et al., 2007; Yttri et al. 2011a), whereas the great diversity of PBAP likely is underestimated by just accounting for plant debris and fungal spores. The lower estimate of OC_{BSOA} and the higher estimate of OC_{PBAP} provided by PMF in the present study is in line with this and encourage further effort to apportion these major carbonaceous aerosol sources correctly. Inclusion of

649   monoterpene and sesquiterpene oxidation products (Kleindienst et al., 2007) to PMF would possibly

650   improve our understanding of the SOA apportionment, as would knowledge about their atmospheric

651   lifetime.

652

653   **4. Conclusions**

654   The carbonaceous aerosol time-series at the Birkenes Observatory initiated in 2001 is unique due to its

655   unprecedented length in Europe and because measurements are performed both for PM_{10} and $PM_{2.5}$.

656   Such long-time series are of utmost importance, e.g. for the evaluation of projections, air-quality models,

657   and climate models. The need for concurrent and diverse off-line and on-line carbonaceous aerosol

658   speciation measurements for understanding of carbonaceous aerosol sources, seasonal, annual, and long-

659   term variability has been utterly demonstrated.

660   Statistically significant and comparably large reductions ($\sim$ -4% yr^{-1}) were calculated for EC

661   and $PM_{2.5}$ at the Birkenes Observatory for 2001–2018, with EC reductions largely attributed to road

662   transportation. No significant declining trend was calculated for OC, likely because prevailing natural

663   sources masked any reduction in anthropogenic sources. Further reduction of carbonaceous aerosol may

664   be hampered by poorly abated sources such as domestic heating, though more work is needed to assess

665   this. We emphasize the importance of establishing long lasting, high quality carbonaceous aerosol and

666   organic tracers time series at several sites across Europe for this purpose. The OC fraction of PM_{10}

667   (+2.3% yr^{-1}) and $PM_{2.5}$ (+3.2% yr^{-1}) increased significantly from 2001–2018, whereas the EC fraction

668   decreased (-4.0 – -4.7% yr^{-1}), causing a successive change in the aerosol chemical composition and in

669   the relative source composition.

670   Source apportionment using PMF identified seven factors, six of which were carbonaceous

671   dominated: Mineral dust dominated (MIN), traffic/industrial-like (TRA/IND), biogenic secondary

672   organic aerosol (BSOA), primary biological aerosol particles (PBAP), biomass burning (BB) and

673   ammonium nitrate dominated (NH_4NO_3). Carbonaceous material was negligible in the sea salt (SS)

674   factor. Combustion of fossil fuel (78%) was the major source of EC and TRA/IND (50%) the key factor.

675   Emissions from residential wood burning increased in the heating season but fossil fuel sources

676   dominated EC even in winter (66%). Continental Europe and western parts of Russia were the main

677   source regions of elevated levels of eBC, both for biomass burning and for combustion of fossil fuels.

678   Natural sources dominated both fine (53%) and coarse (78%) fraction OC, thus also OC in PM_{10} (60%).

679   The natural fraction increased substantially in the vegetative season due to biogenic secondary organic

680   aerosol and primary biological aerosol particles, confined to the BSOA, PBAP and MIN factors. 77–

681   91% of OC was attributed to natural sources in summer and 22–37% in winter. The coarse fraction

682   showed the highest share of natural sources regardless of season and was dominated by PBAP, except

683   in winter. Notably, PBAP (26%) made a larger contribution to OC in PM_{10} than BB (14%), and an

684   equally large contribution as BB (17%) in $PM_{2.5}$.

19

References

Aas, W., Eckhardt, S., Fiebig, M., Solberg, S., and Yttri, K. E.: Monitoring of long-range transported air pollutants in Norway, annual report 2019. Kjeller, NILU (Miljødirektoratet rapport, M-1710/2020)

721   (NILU OR, 4/2020), 2020.

722   Alastuey, A., Querol, X., Aas, W., Lucarelli, F., Perez, N., Moreno, T., Cavalli, F., Areskoug, H., Balan,

723   V., Catrambone, M., Ceburnis, D., Cerro, J. C., Conil, S., Gevorgyan, L., Hueglin, C., Imre, K., Jaffrezo,

724   J.-L., Leeson, S. R., Mihalopoulos, N., Mitosinkova, M., O'Dowd, C. D., Pey, J., Putaud, J.-P., Riffault,

725   V., Ripoll, A., Sciare, J., Sellegri, K., Spindler, G., and Yttri, K. E.: Geochemistry of PM_{10} over Europe

726   during the EMEP intensive measurement periods in summer 2012 and winter 2013, Atmos. Chem.

727   Phys., 16, 6107-6129, 10.5194/acp-16-6107-2016, 2016.

728   Amundsen, C. E., Hanssen, J. E., Semb, A., and Steinnes, E.: Long-range atmospheric transport of trace

729   elements to Southern Norway, Atmos. Environ., Part a-General Topics, 26, 1309-1324, 10.1016/0960-

730   1686(92)90391-w, 1992.

731   Bauer, H., Claeys, M., Vermeylen, R., Schueller, E., Weinke, G., Berger, A., and Puxbaum, H.: Arabitol

732   and mannitol as tracers for the quantification of airborne fungal spores, Atmos. Environ, 42, 588-593,

733   10.1016/j.atmosenv.2007.10.013, 2008.

734   Bauer, H., Kasper-Giebl, A., Loflund, M., Giebl, H., Hitzenberger, R., Zibuschka, F., and Puxbaum, H.:

735   The contribution of bacteria and fungal spores to the organic carbon content of cloud water, precipitation

736   and aerosols, Atmos. Res., 64, 109-119, 10.1016/s0169-8095(02)00084-4, 2002.

737   Bergstrom, R., van der Gon, H. A. C. D., Prevot, A. S. H., Yttri, K. E., and Simpson, D.: Modelling of

738   organic aerosols over Europe (2002-2007) using a volatility basis set (VBS) framework: application of

739   different assumptions regarding the formation of secondary organic aerosol, Atmos. Chem. Phys., 12,

740   8499-8527, 10.5194/acp-12-8499-2012, 2012.

741   Bond, T. C., Doherty, S. J., Fahey, D. W., Forster, P. M., Berntsen, T., DeAngelo, B. J., Flanner, M. G.,

742   Ghan, S., Karcher, B., Koch, D., Kinne, S., Kondo, Y., Quinn, P. K., Sarofim, M. C., Schultz, M. G.,

743   Schulz, M., Venkataraman, C., Zhang, H., Zhang, S., Bellouin, N., Guttikunda, S. K., Hopke, P. K.,

744   Jacobson, M. Z., Kaiser, J. W., Klimont, Z., Lohmann, U., Schwarz, J. P., Shindell, D., Storelvmo, T.,

745   Warren, S. G., and Zender, C. S.: Bounding the role of black carbon in the climate system: A scientific

746   assessment, J. Geophys. Res.-Atmos., 118, 5380-5552, 10.1002/jgrd.50171, 2013.

747   Boucher, O., Randall, D., Artaxo, P., Bretherton, C., Feingold, G., Forster, P., Kerminen, V.-M.,

748   Kondo, Y., Liao, H., Lohmann, U., Rasch, P., Satheesh, S. K., Sherwood, S., Stevens, B., and Zhang,

749   X.Y.: Clouds and Aerosols. In: Climate Change 2013: The Physical Science Basis. Contribution of

750   Working Group I to the Fifth Assessment Report of the Intergovernmental Panel on Climate Change

751   [Stocker, T.F., Qin, D., Plattner, G. K., Tignor, M., Allen, S. K., Boschung, J., Nauels, A., Xia, Y.,

752   Bex, V., and Midgley, P. M. (eds.)]: Cambridge University Press, Cambridge, United Kingdom and

753   New York, NY, USA, 2013.

754   Bougiatioti, A., Stavroulas, I., Kostenidou, E., Zarmpas, P., Theodosi, C., Kouvarakis, G., Canonaco,

755   F., Prevot, A. S. H., Nenes, A., Pandis, S. N., and Mihalopoulos, N.: Processing of biomass-burning

756   aerosol in the eastern Mediterranean during summertime, Atmos. Chem. Phys., 14, 4793-4807,

757   10.5194/acp-14-4793-2014, 2014.

758   Canonaco, F., Crippa, M., Slowik, J. G., Baltensperger, U., and Prevot, A. S. H.: SoFi, an IGOR-based

759   interface for the efficient use of the generalized multilinear engine (ME-2) for the source apportionment:

760   ME-2 application to aerosol mass spectrometer data, Atmos. Meas. Tech., 6, 3649-3661, 10.5194/amt-

761   6-3649-2013, 2013.

762   Carvalho, A., Pio, C., and Santos, C.: Water-soluble hydroxylated organic compounds in German and

763   Finnish aerosols, Atmos. Environ., 37, 1775-1783, 10.1016/s1352-2310(03)00066-9, 2003.

764   Cassiani, M., Stohl, A., and Brioude, J.: Lagrangian Stochastic Modelling of Dispersion in the

765   Convective Boundary Layer with Skewed Turbulence Conditions and a Vertical Density Gradient:

766   Formulation and Implementation in the FLEXPART Model, Bound-Lay Meteorol, 154, 367-390,

767   10.1007/s10546-014-9976-5, 2015.

768   Cavalli, F., Viana, M., Yttri, K. E., Genberg, J., and Putaud, J.-P.: Toward a standardised thermal-optical

769   protocol for measuring atmospheric organic and elemental carbon: the EUSAAR protocol, Atmos.

770   Meas. Tech., 3, 79-89, 2010.

771   Cavalli, C., Putaud, J.P., Yttri, K.E. Availability and quality of the EC and OC measurements within

772   EMEP, including results of the fourth interlaboratory comparison of analytical methods for

773   carbonaceous particulate matter within EMEP (2011). EMEP/CCC-Report 1/2013.

774   Claeys, M., Graham, B., Vas, G., Wang, W., Vermeylen, R., Pashynska, V., Cafmeyer, J., Guyon, P.,

775   Andreae, M. O., Artaxo, P., and Maenhaut, W.: Formation of secondary organic aerosols through

776   photooxidation of isoprene, Science., 303, 1173-1176, 10.1126/science.1092805, 2004.

777   Crippa, M., Canonaco, F., Lanz, V. A., Aijala, M., Allan, J. D., Carbone, S., Capes, G., Ceburnis, D.,

778   Dall'Osto, M., Day, D. A., DeCarlo, P. F., Ehn, M., Eriksson, A., Freney, E., Hildebrandt Ruiz, L.,

779   Hillamo, R., Jimenez, J. L., Junninen, H., Kiendler-Scharr, A., Kortelainen, A. M., Kulmala, M.,

780   Laaksonen, A., Mensah, A., Mohr, C., Nemitz, E., O'Dowd, C., Ovadnevaite, J., Pandis, S. N., Petaja,

781   T., Poulain, L., Saarikoski, S., Sellegri, K., Swietlicki, E., Tiitta, P., Worsnop, D. R., Baltensperger, U.,

782   and Prevot, A. S. H.: Organic aerosol components derived from 25 AMS data sets across Europe using

783   a consistent ME-2 based source apportionment approach, Atmos. Chem. Phys., 14, 6159-6176,

784   10.5194/acp-14-6159-2014, 2014.

785   Donahue, N. M., Robinson, A. L., and Pandis, S. N.: Atmospheric organic particulate matter: From

786   smoke to secondary organic aerosol, Atmos. Environ., 43, 94-106, 10.1016/j.atmosenv.2008.09.055,

787   2009.

788   Dusek, U., Hitzenberger, R., Kasper-Giebl, A., Kistler, M., Meijer, H. A. J., Szidat, S., Wacker, L.,

789   Holzinger, R., and Rockmann, T.: Sources and formation mechanisms of carbonaceous aerosol at a

790   regional background site in the Netherlands: insights from a year-long radiocarbon study, Atmos. Chem.

791   Phys., 17, 3233-3251, 10.5194/acp-17-3233-2017, 2017.

792   Dye, C. and Yttri, K.: Determination of monosaccharide anhydrides in atmospheric aerosols by use of

793   high-performance liquid chromatography combined with high-resolution mass spectrometry, Anal.

794   Chem., 77, 1853-1858, 10.1021/ac049461j, 2005.

795   EEA, 2021: Long term air quality measurements trends in Europe. In prep.

796   Elbert, W., Taylor, P. E., Andreae, M. O., and Poschl, U.: Contribution of fungi to primary biogenic

797   aerosols in the atmosphere: wet and dry discharged spores, carbohydrates, and inorganic ions, Atmos.

798   Chem. Phys., 7, 4569-4588, 10.5194/acp-7-4569-2007, 2007.

799   Fomba, K. W., van Pinxteren, D., Muller, K., Spindler, G., and Herrmann, H.: Assessment of trace metal

800   levels in size-resolved particulate matter in the area of Leipzig, Atmos. Environ., 176, 60-70,

801   10.1016/j.atmosenv.2017.12.024, 2018.

802   Forster, C., Stohl, A., and Seibert, P.: Parameterization of convective transport in a Lagrangian particle

803   dispersion model and its evaluation, J. Appl. Meteorol. Clim., 46, 403-422, 10.1175/jam2470.1, 2007.

804   Frohlich-Nowoisky, J., Kampf, C. J., Weber, B., Huffman, J. A., Pohlker, C., Andreae, M. O., Lang-

805   Yona, N., Burrows, S. M., Gunthe, S. S., Elbert, W., Su, H., Hoor, P., Thines, E., Hoffmann, T., Despres,

806   V. R., and Poschl, U.: Bioaerosols in the Earth system: Climate, health, and ecosystem interactions,

807   Atmos. Res., 182, 346-376, 10.1016/j.atmosres.2016.07.018, 2016.

808   Fuller, G. W., Tremper, A. H., Baker, T. D., Yttri, K. E., and Butterfield, D.: Contribution of wood

809   burning to PM_{10} in London, Atmos. Environ., 87, 87-94, 10.1016/j.atmosenv.2013.12.037, 2014.

810   Gelencser, A., May, B., Simpson, D., Sanchez-Ochoa, A., Kasper-Giebl, A., Puxbaum, H., Caseiro, A.,

811   Pio, C., and Legrand, M.: Source apportionment of $PM_{2.5}$ organic aerosol over Europe:

812   Primary/secondary, natural/anthropogenic, and fossil/biogenic origin, J. Geophys. Res.-Atmos., 112,

813   10.1029/2006jd008094, 2007.

814   Genberg, J., Hyder, M., Stenstrom, K., Bergstrom, R., Simpson, D., Fors, E. O., Jonsson, J. A., and

815   Swietlicki, E.: Source apportionment of carbonaceous aerosol in southern Sweden, Atmos. Chem. Phys.,

816   11, 11387-11400, 10.5194/acp-11-11387-2011, 2011.

817   Gilbert, R. O.: Statistical Methods for Environmental Pollution Monitoring, Wiley, NY, United States,

818   pp. 336, 1987.

819   Gilardoni, S., Vignati, E., Cavalli, F., Putaud, J. P., Larsen, B. R., Karl, M., Stenstrom, K., Genberg, J.,

820   Henne, S., and Dentener, F.: Better constraints on sources of carbonaceous aerosols using a combined

821   C-14 - macro tracer analysis in a European rural background site, Atmos. Chem. Phys., 11, 5685-5700,

822   10.5194/acp-11-5685-2011, 2011.

823   Glasius, M., Hansen, A. M. K., Claeys, M., Henzing, J. S., Jedynska, A. D., Kasper-Giebl, A., Kistler,

824   M., Kristensen, K., Martinsson, J., Maenhaut, W., Nojgaard, J. K., Spindler, G., Stenstrom, K. E.,

825   Swietlicki, E., Szidat, S., Simpson, D., and Yttri, K. E.: Composition and sources of carbonaceous

826   aerosols in Northern Europe during winter, Atmos. Environ., 173, 127-141,

827   10.1016/j.atmosenv.2017.11.005, 2018.

828   Grythe, H., Kristiansen, N. I., Zwaaftink, C. D. G., Eckhardt, S., Strom, J., Tunved, P., Krejci, R., and

829   Stohl, A.: A new aerosol wet removal scheme for the Lagrangian particle model FLEXPART v10,

830   Geosci. Model Dev., 10, 1447-1466, 10.5194/gmd-10-1447-2017, 2017.

831   Grythe, H., Lopez-Aparicio, S., Vogt, M., Thanh, D. V., Hak, C., Halse, A. K., Hamer, P., and Santos,

832   G. S.: The MetVed model: development and evaluation of emissions from residential wood combustion

833   at high spatio-temporal resolution in Norway, Atmos. Chem. Phys., 19, 10.5194/acp-19-10217-2019,

834   2019.

835   Hallquist, M., Wenger, J. C., Baltensperger, U., Rudich, Y., Simpson, D., Claeys, M., Dommen, J.,

836   Donahue, N. M., George, C., Goldstein, A. H., Hamilton, J. F., Herrmann, H., Hoffmann, T., Iinuma,

837   Y., Jang, M., Jenkin, M. E., Jimenez, J. L., Kiendler-Scharr, A., Maenhaut, W., McFiggans, G., Mentel,

838   T. F., Monod, A., Prevot, A. S. H., Seinfeld, J. H., Surratt, J. D., Szmigielski, R., and Wildt, J.: The

839   formation, properties and impact of secondary organic aerosol: current and emerging issues, Atmos.

840   Chem. Phys., 9, 5155-5236, 10.5194/acp-9-5155-2009, 2009.

841 Herich, H., Gianini, M. F. D., Piot, C., Mocnik, G., Jaffrezo, J. L., Besombes, J. L., Prevot, A. S. H.,
842 and Hueglin, C.: Overview of the impact of wood burning emissions on carbonaceous aerosols and PM
843 in large parts of the Alpine region, Atmos. Environ., 89, 64-75, 10.1016/j.atmosenv.2014.02.008, 2014.

844 Hirdman, D., Sodemann, H., Eckhardt, S., Burkhart, J. F., Jefferson, A., Mefford, T., Quinn, P. K.,
845 Sharma, S., Strom, J., and Stohl, A.: Source identification of short-lived air pollutants in the Arctic using
846 statistical analysis of measurement data and particle dispersion model output, Atmos. Chem. Phys., 10,
847 669-693, 10.5194/acp-10-669-2010, 2010.

848 Hjellbrekke, A-G.: Data Report 2018. Particulate matter, carbonaceous and inorganic compounds,
849 NILU, Kjeller, EMEP/CCC-Report 1/2020, 2020.

850 Hodnebrog, O., Myhre, G., and Samset, B. H.: How shorter black carbon lifetime alters its climate effect,
851 Nat. Commun., 5, 10.1038/ncomms6065, 2014.

852 Hoffmann, D., Tilgner, A., Iinuma, Y., and Herrmann, H.: Atmospheric Stability of Levoglucosan: A
853 Detailed Laboratory and Modeling Study, Environ. Sci. Technol., 44, 694-699, 10.1021/es902476f,
854 2010a.

855 Hoffmann, D., Tilgner, A., Iinuma, Y., and Herrmann, H.: Atmospheric Stability of Levoglucosan: A
856 Detailed Laboratory and Modeling Study, Environ. Sci. Technol, 44, 694-699, 10.1021/es902476f,
857 2010b.

858 Janssen, N. A. H., Gerlofs-Nijland, M. E., Lanki, T., Salonen, R. O., Cassee, F., Hoek, G., Fischer, P.,
859 Brunekreef, B., and Krzyzanowski, M.: Health effects of black carbon. Copenhagen: WHO Regional
860 Office for Europe, 2012.

861 Jia, Y. L. and Fraser, M.: Characterization of Saccharides in Size-fractionated Ambient Particulate
862 Matter and Aerosol Sources: The Contribution of Primary Biological Aerosol Particles (PBAPs) and
863 Soil to Ambient Particulate Matter, Environ. Sci. Technol., 45, 930-936, 10.1021/es103104e, 2011.

864 Kahnert, M., Lazaridis, M., Tsyro, S., and Torseth, K.: Requirements for developing a regional
865 monitoring capacity for aerosols in Europe within EMEP, J. Environ. Monitor., 6, 646-655,
866 10.1039/b315136k, 2004.

867 Kendall, M. G.: Rank correlation methods, 4th edition, Charles Griffin, London, 1975.

868 Kleindienst, T. E., Jaoui, M., Lewandowski, M., Offenberg, J. H., Lewis, C. W., Bhave, P. V., and
869 Edney, E. O.: Estimates of the contributions of biogenic and anthropogenic hydrocarbons to secondary

870 organic aerosol at a southeastern US location, Atmos. Environ., 41, 8288-8300,
871 10.1016/j.atmosenv.2007.06.045, 2007.

872 Kocbach, A., Li, Y. J., Yttri, K. E., Cassee, F. R., Schwarze, P. E., and Namork, E.: Physicochemical
873 characterisation of combustion particles from vehicle exhaust and residential wood smoke, Part. Fibre
874 Toxicol., 3, 10.1186/1743-8977-3-1, 2006.

875 Kyllonen, K., Vestenius, M., Anttila, P., Makkonen, U., Aurela, M., Wangberg, I., Mastromonaco, M.
876 N., and Hakola, H.: Trends and source apportionment of atmospheric heavy metals at a subarctic site
877 during 1996-2018, Atmos. Environ., 236, 10.1016/j.atmosenv.2020.117644, 2020.

878 Lanz, V. A., Prevot, A. S. H., Alfarra, M. R., Weimer, S., Mohr, C., DeCarlo, P. F., Gianini, M. F. D.,
879 Hueglin, C., Schneider, J., Favez, O., D'Anna, B., George, C., and Baltensperger, U.: Characterization
880 of aerosol chemical composition with aerosol mass spectrometry in Central Europe: an overview,
881 Atmos. Chem. Phys., 10, 10453-10471, 10.5194/acp-10-10453-2010, 2010.

882 Lund, M. T., Myhre, G., Haslerud, A. S., Skeie, R. B., Griesfeller, J., Platt, S. M., Kumar, R., Myhre,
883 C. L., and Schulz, M.: Concentrations and radiative forcing of anthropogenic aerosols from 1750 to
884 2014 simulated with the Oslo CTM3 and CEDS emission inventory, Geosci. Model Dev., 11, 4909-
885 4931, 10.5194/gmd-11-4909-2018, 2018.

886 Maenhaut, W.: Source apportionment revisited for long-term measurements of fine aerosol trace
887 elements at two locations in southern Norway, Nucl. Instrum. Meth. B., 417, 133-138,
888 10.1016/j.nimb.2017.07.006, 2018.

889 Maenhaut, W., Vermeylen, R., Claeys, M., Vercauteren, J., Matheeussen, C., and Roekens, E.:
890 Assessment of the contribution from wood burning to the PM_{10} aerosol in Flanders, Belgium, Sci. Tot.
891 Environ., 437, 226-236, 10.1016/j.scitotenv.2012.08.015, 2012.

892 Malm, W.C., Sisler, J.F., Huffmann, D., Eldred, R.A., Cahill, T.A.: Spatial and seasonal trends in
893 particles concentrations and optical extinction in the United-States. J. Geophys. Res. 99(D1), 1347-
894 1370, 1994.
895 Mann, H. B.: Non-parametric tests against trend, Econometrica 13:163-171, 1945.

896 Matthews, B., Mareckova, K., Schindlbacher, S., Ullrich, B., and Wankmwüller, R.: Emissions for 2018,
897 in: Transboundary particulate matter, photo-oxidants, acidifying and eutrophying components. EMEP
898 Status Report 1/2020, pp. 37-57, The Norwegian Meteorological Institute, Oslo, Norway, 2020.

899   Myhre, G. and Samset, B. H.: Standard climate models radiation codes underestimate black carbon

900   radiative forcing, Atmos. Chem. Phys., 15, 2883-2888, 10.5194/acp-15-2883-2015, 2015.

901   Myhre, G., Shindell, D., Bréon, F.-M., Collins, W., Fuglestvedt, J., Huang, J., Koch, D., Lamarque, J.-

902   F., Lee, D., Mendoza, B., Nakajima, T., Robock, A., Stephens, G., Takemura, T., and Zhang, H.:

903   Anthropogenic and Natural Radiative Forcing. In: Climate Change 2013: The Physical Science Basis.

904   Contribution of Working Group I to the Fifth Assessment Report of the Intergovernmental Panel on

905   Climate Change [Stocker, T.F., Qin, D., Plattner, G.-K., Tignor, M., Allen, S.K., Boschung, J., Nauels,

906   A., Xia, Y., Bex, V., and Midgley, P.M. (eds.)], Cambridge University Press, Cambridge, United

907   Kingdom and New York, NY, USA, 2013.

908   Norris, G., Duvall, R., Brown, S., and Bai, S.: EPA Positive Matrix Factorization (PMF) 5.0

909   Fundamentals and User Guide, U.S. Environmental Protection Agency, Washington, DC, 20460 (i-124,

910   EPA/600/R-14/108, April), 2014.

911   O'Dowd, C. D., Facchini, M. C., Cavalli, F., Ceburnis, D., Mircea, M., Decesari, S., Fuzzi, S., Yoon, Y.

912   J., and Putaud, J. P.: Biogenically driven organic contribution to marine aerosol, Nature, 431, 676-680,

913   10.1038/nature02959, 2004.

914   Pacyna, J. M., Nriagu, J. O., Davidson, C. I. (Eds.): Toxic Metals in the Atmosphere, Wiley, New York,

915   USA, (1986).

916   Pio, C. A., Legrand, M., Oliveira, T., Afonso, J., Santos, C., Caseiro, A., Fialho, P., Barata, F., Puxbaum,

917   H., Sanchez-Ochoa, A., Kasper-Giebl, A., Gelencser, A., Preunkert, S., and Schock, M.: Climatology

918   of aerosol composition (organic versus inorganic) at nonurban sites on a west-east transect across

919   Europe, J. Geophys. Res.-Atmos., 112, 10.1029/2006jd008038, 2007.

920   Pisso, I., Sollum, E., Grythe, H., Kristiansen, N. I., Cassiani, M., Eckhardt, S., Arnold, D., Morton, D.,

921   Thompson, R. L., Zwaaftink, C. D. G., Evangeliou, N., Sodemann, H., Haimberger, L., Henne, S.,

922   Brunner, D., Burkhart, J. F., Fouilloux, A., Brioude, J., Philipp, A., Seibert, P., and Stohl, A.: The

923   Lagrangian particle dispersion model FLEXPART version 10.4, Geosci. Model Dev., 12, 4955-4997,

924   10.5194/gmd-12-4955-2019, 2019.

925   Polissar, A. V., Hopke, P. K., and Paatero, P.: Atmospheric aerosol over Alaska - 2. Elemental

926   composition and sources, J. Geophys. Res.-Atmos., 103, 19045-19057, 10.1029/98jd01212, 1998.

927   Puxbaum, H., Caseiro, A., Sanchez-Ochoa, A., Kasper-Giebl, A., Claeys, M., Gelencser, A., Legrand,

928   M., Preunkert, S., and Pio, C.: Levoglucosan levels at background sites in Europe for assessing the

929   impact of biomass combustion on the European aerosol background, J. Geophys. Res.-Atmos., 112,

930   10.1029/2006jd008114, 2007.

931   Reis, S., Grennfelt, P., Klimont, Z., Amann, M., ApSimon, H., Hettelingh, J. P., Holland, M., LeGall,

932   A. C., Maas, R., Posch, M., Spranger, T., Sutton, M. A., and Williams, M.: From Acid Rain to Climate

933   Change, Science, 338, 1153-1154, 10.1126/science.1226514, 2012.

934   Ripoll, A., Minguillon, M. C., Pey, J., Perez, N., Querol, X., and Alastuey, A.: Joint analysis of

935   continental and regional background environments in the western Mediterranean: PM_1 and PM_{10}

936   concentrations and composition, Atmos. Chem. Phys., 15, 1129-1145, 10.5194/acp-15-1129-2015,

937   2015.

938   Rogge, W. F., Hildemann, L. M., Mazurek, M. A., Cass, G. R., and Simonelt, B. R. T.: SOURCES OF

939   FINE ORGANIC AEROSOL .1. CHARBROILERS AND MEAT COOKING OPERATIONS,

940   Environ. Sci. Technol., 25, 1112-1125, 10.1021/es00018a015, 1991.

941   Rotzer, T. and Chmielewski, F. M.: Phenological maps of Europe, Clim. Res., 18, 249-257,

942   10.3354/cr018249, 2001.

943   Saarikoski, S., Timonen, H., Saarnio, K., Aurela, M., Jarvi, L., Keronen, P., Kerminen, V. M., and

944   Hillamo, R.: Sources of organic carbon in fine particulate matter in northern European urban air, Atmos.

945   Chem. Phys., 8, 6281-6295, 10.5194/acp-8-6281-2008, 2008.

946   Saffari, A., Daher, N., Samara, C., Voutsa, D., Kouras, A., Manoli, E., Karagkiozidou, O., Vlachokostas,

947   C., Moussiopoulos, N., Shafer, M. M., Schauer, J. J., and Sioutas, C.: Increased Biomass Burning Due

948   to the Economic Crisis in Greece and Its Adverse Impact on Wintertime Air Quality in Thessaloniki,

949   Environ. Sci. Technol., 47, 13313-13320, 10.1021/es403847h, 2013.

950   Samake, A., Bonin, A., Jaffrezo, J. L., Taberlet, P., Weber, S., Uzu, G., Jacob, V., Conil, S., and Martins,

951   J. M. F.: High levels of primary biogenic organic aerosols are driven by only a few plant-associated

952   microbial taxa, Atmos. Chem. Phys., 20, 5609-5628, 10.5194/acp-20-5609-2020, 2020.

953   Samake, A., Jaffrezo, J. L., Favez, O., Weber, S., Jacob, V., Canete, T., Albinet, A., Charron, A.,

954   Riffault, V., Perdrix, E., Waked, A., Golly, B., Salameh, D., Chevrier, F., Oliveira, D. M., Besombes, J.

955   L., Martins, J. M. F., Bonnaire, N., Conil, S., Guillaud, G., Mesbah, B., Rocq, B., Robic, P. Y., Hulin,

956   A., Le Meur, S., Descheemaecker, M., Chretien, E., Marchand, N., and Uzu, G.: Arabitol, mannitol, and

957   glucose as tracers of primary biogenic organic aerosol: the influence of environmental factors on

958   ambient air concentrations and spatial distribution over France, Atmos. Chem. Phys., 19, 11013-11030,

959   10.5194/acp-19-11013-2019, 2019.

Sandradewi, J., Prevot, A. S. H., Szidat, S., Perron, N., Alfarra, M. R., Lanz, V. A., Weingartner, E., and Baltensperger, U.: Using aerosol light absorption measurements for the quantitative determination of wood burning and traffic emission contributions to particulate matter, Environ. Sci. Technol., 42, 3316-3323, 10.1021/es702253m, 2008.

Sciare, J., Oikonomou, K., Favez, O., Liakakou, E., Markaki, Z., Cachier, H., and Mihalopoulos, N.: Long-term measurements of carbonaceous aerosols in the Eastern Mediterranean: evidence of long-range transport of biomass burning, Atmos. Chem. Phys., 8, 5551-5563, 10.5194/acp-8-5551-2008, 2008.

Sen, P. K.: Estimates of the regression coefficient based on Kendall's Tau. J. Am., Stat. Assoc. 63 (324), 1379–1389.https://doi.org/10.2307/2285891, 1968.

Sillanpaa, M., Frey, A., Hillamo, R., Pennanen, A. S., and Salonen, R. O.: Organic, elemental and inorganic carbon in particulate matter of six urban environments in Europe, Atmos. Chem. Phys., 5, 2869-2879, 10.5194/acp-5-2869-2005, 2005.

Simpson, D., Yttri, K. E., Klimont, Z., Kupiainen, K., Caseiro, A., Gelencser, A., Pio, C., Puxbaum, H., and Legrand, M.: Modeling carbonaceous aerosol over Europe: Analysis of the CARBOSOL and EMEP EC/OC campaigns, J. Geophys. Res.-Atmos., 112, 10.1029/2006JD008158, 2007.

Simpson, D., Bergström, R., Denier van der Gon, H., Kuenen, J., Schindlbacher, S., and Visschedijk, A.: Condensable organics; issues and implications for EMEP calculations and source-receptor matrices, in: Transboundary particulate matter, photo-oxidants, acidifying and eutrophying components. EMEP Status Report 1/2019, pp. 71-88, The Norwegian Meteorological Institute, Oslo, Norway, 2019.

Skjoth, C. A., Sommer, J., Stach, A., Smith, M., and Brandt, J.: The long-range transport of birch (Betula) pollen from Poland and Germany causes significant pre-season concentrations in Denmark, Clin. Exp. Allergy, 37, 1204-1212, 10.1111/j.1365-2222.2007.02771.x, 2007.

Sofiev, M., Siljamo, P., Ranta, H., and Rantio-Lehtimaki, A.: Towards numerical forecasting of long-range air transport of birch pollen: theoretical considerations and a feasibility study, Int. J. Biometeorol., 50, 392-402, 10.1007/s00484-006-0027-x, 2006.

Spracklen, D. V., Jimenez, J. L., Carslaw, K. S., Worsnop, D. R., Evans, M. J., Mann, G. W., Zhang, Q., Canagaratna, M. R., Allan, J., Coe, H., McFiggans, G., Rap, A., and Forster, P.: Aerosol mass spectrometer constraint on the global secondary organic aerosol budget, Atmos. Chem. Phys., 11, 12109-12136, 10.5194/acp-11-12109-2011, 2011.

990 Stohl, A., Forster, C., Frank, A., Seibert, P., and Wotawa, G.: Technical note: The Lagrangian particle
991 dispersion model FLEXPART version 6.2, Atmos. Chem. Phys., 5, 2461-2474, 10.5194/acp-5-2461-
992 2005, 2005.

993 Stohl, A., Andrews, E., Burkhart, J. F., Forster, C., Herber, A., Hoch, S. W., Kowal, D., Lunder, C.,
994 Mefford, T., Ogren, J. A., Sharma, S., Spichtinger, N., Stebel, K., Stone, R., Strom, J., Torseth, K.,
995 Wehrli, C., and Yttri, K. E.: Pan-Arctic enhancements of light absorbing aerosol concentrations due to
996 North American boreal forest fires during summer 2004, J. Geophys. Res.-Atmos., 111,
997 10.1029/2006JD007216, 2006.

998 Stohl, A., Berg, T., Burkhart, J. F., Fjaeraa, A. M., Forster, C., Herber, A., Hov, O., Lunder, C.,
999 McMillan, W. W., Oltmans, S., Shiobara, M., Simpson, D., Solberg, S., Stebel, K., Strom, J., Torseth,
1000 K., Treffeisen, R., Virkkunen, K., and Yttri, K. E.: Arctic smoke - record high air pollution levels in the
1001 European Arctic due to agricultural fires in Eastern Europe in spring 2006, Atmos. Chem. Phys., 7, 511-
1002 534, 2007.

1003 Stumm, W. and Morgan, J. J. (eds.): Aquatic Chemistry: Chemical Equilibria and Rates in Natural
1004 Waters, 3rd Edition, Wiley-Interscience Series of Texts and Monographs, Wiley, New York, 1996.

1005 Szidat, S., Prevot, A. S. H., Sandradewi, J., Alfarra, M. R., Synal, H. A., Wacker, L., and Baltensperger,
1006 U.: Dominant impact of residential wood burning on particulate matter in Alpine valleys during winter,
1007 Geophys. Res. Lett., 34, 10.1029/2006gl028325, 2007.

1008 Szidat, S., Ruff, M., Perron, N., Wacker, L., Synal, H.-A., Hallquist, M., Shannigrahi, A. S., Yttri, K.
1009 E., Dye, C., and Simpson, D.: Fossil and non-fossil sources of organic carbon (OC) and elemental carbon
1010 (EC) in Goteborg, Sweden, Atmos. Chem. Phys., 9, 1521-1535, 10.5194/acp-9-1805-2009, 2009.

1011 Theil, H.: A rank-invariant method of linear and polynomial regression analysis. Proc. R. Netherlands,
1012 Acad. Sci. 53, 386–392, https://doi.org/10.1007/978-94-011-2546-8_20, 1950.

1013 Tørseth, K. and Hov, Ø. (eds.): The EMEP monitoring strategy 2004-2009. Background document with
1014 justification and specification of the EMEP monitoring programme 2004-2009, Kjeller, NILU
1015 (EMEP/CCC, 09/2003), 2003.

1016 Torseth, K., Aas, W., Breivik, K., Fjaeraa, A. M., Fiebig, M., Hjellbrekke, A. G., Myhre, C. L., Solberg,
1017 S., and Yttri, K. E.: Introduction to the European Monitoring and Evaluation Programme (EMEP) and
1018 observed atmospheric composition change during 1972-2009, Atmos. Chem. Phys., 12, 5447-5481,
1019 10.5194/acp-12-5447-2012, 2012.

1020   Trebs, I., Andreae, M. O., Elbert, W., Mayol-Bracero, O. L., Soto-Garcia, L. L., Rudich, Y., Falkovich,
1021   A. H., Maenhaut, W., Artaxo, P., Otjes, R., and Slanina, J.: Aerosol inorganic composition at a tropical
1022   site: Discrepancies between filter-based sampling and a semi-continuous method, Aerosol Sci. Tech,
1023   42, 255-269, 10.1080/02786820801992899, 2008.

1024   UNECE: 1999 Protocol to Abate Acidification, Eutrophication and Ground-level Ozone to the
1025   Convention on Long-range Transboundary Air Pollution, as amended on 4 May 2012, Geneva: UNECE,
1026   2013.

1027   UNECE: Monitoring strategy for the Cooperative Programme for Monitoring and Evaluation of the
1028   Long-range Transmission of Air Pollutants in Europe for the period 2020–2029, UNECE, Geneva,
1029   Decision 2019/1, ECE/EB.AIR/144/Add.1, 2019.

1030   van der Gon, H., Bergstrom, R., Fountoukis, C., Johansson, C., Pandis, S. N., Simpson, D., and
1031   Visschedijk, A. J. H.: Particulate emissions from residential wood combustion in Europe revised
1032   estimates and an evaluation, Atmos. Chem. Phys., 15, 6503-6519, 10.5194/acp-15-6503-2015, 2015.

1033   Viana, M., Kuhlbusch, T. A. J., Querol, X., Alastuey, A., Harrison, R. M., Hopke, P. K., Winiwarter,
1034   W., Vallius, A., Szidat, S., Prevot, A. S. H., Hueglin, C., Bloemen, H., Wahlin, P., Vecchi, R., Miranda,
1035   A. I., Kasper-Giebl, A., Maenhaut, W., and Hitzenberger, R.: Source apportionment of particulate matter
1036   in Europe: A review of methods and results, J. Aerosol Sci., 39, 827-849,
1037   10.1016/j.jaerosci.2008.05.007, 2008.

1038   Waked, A., Favez, O., Alleman, L. Y., Piot, C., Petit, J. E., Delaunay, T., Verlinden, E., Golly, B.,
1039   Besombes, J. L., Jaffrezo, J. L., and Leoz-Garziandia, E.: Source apportionment of PM_{10} in a north-
1040   western Europe regional urban background site (Lens, France) using positive matrix factorization and
1041   including primary biogenic emissions, Atmos. Chem. Phys., 14, 3325-3346, 10.5194/acp-14-3325-
1042   2014, 2014.

1043   Weber, S., Salameh, D., Albinet, A., Alleman, L. Y., Waked, A., Besombes, J. L., Jacob, V., Guillaud,
1044   G., Meshbah, B., Rocq, B., Hulin, A., Dominik-Segue, M., Chretien, E., Jaffrezo, J. L., and Favez, O.:
1045   Comparison of PM_{10} Sources Profiles at 15 French Sites Using a Harmonized Constrained Positive
1046   Matrix Factorization Approach, Atmosphere, 10, 10.3390/atmos10060310, 2019.

1047   WHO: Review of evidence on health aspects of air pollution – REVIHAAP Project, Technical Report,
1048   Copenhagen: WHO Regional Office for Europe, 2013.

1049   Yttri, K. E., Aas, W., Bjerke, A., Cape, J. N., Cavalli, F., Ceburnis, D., Dye, C., Emblico, L., Facchini,
1050   M. C., Forster, C., Hanssen, J. E., Hansson, H. C., Jennings, S. G., Maenhaut, W., Putaud, J. P., and

1051 Torseth, K.: Elemental and organic carbon in PM$_{10}$: a one year measurement campaign within the

1052 European Monitoring and Evaluation Programme EMEP, Atmos. Chem. Phys., 7, 5711-5725, 2007a.

1053 Yttri, K. E., Dye, C., and Kiss, G.: Ambient aerosol concentrations of sugars and sugar-alcohols at four

1054 different sites in Norway, Atmos. Chem. Phys., 7, 4267-4279, 2007b.

1055 Yttri, K. E., Simpson, D., Nojgaard, J. K., Kristensen, K., Genberg, J., Stenstrom, K., Swietlicki, E.,

1056 Hillamo, R., Aurela, M., Bauer, H., Offenberg, J. H., Jaoui, M., Dye, C., Eckhardt, S., Burkhart, J. F.,

1057 Stohl, A., and Glasius, M.: Source apportionment of the summer time carbonaceous aerosol at Nordic

1058 rural background sites, Atmos. Chem. Phys., 11, 13339-13357, 10.5194/acp-11-13339-2011, 2011b.

1059 Yttri, K. E., Simpson, D., Stenstrom, K., Puxbaum, H., and Svendby, T.: Source apportionment of the

1060 carbonaceous aerosol in Norway - quantitative estimates based on C-14, thermal-optical and organic

1061 tracer analysis, Atmos. Chem. Phys., 11, 9375-9394, 10.5194/acp-11-9375-2011, 2011a.

1062 Yttri, K. E., Myhre, C. L., Eckhardt, S., Fiebig, M., Dye, C., Hirdman, D., Stroem, J., Klimont, Z., and

1063 Stohl, A.: Quantifying black carbon from biomass burning by means of levoglucosan - a one-year time

1064 series at the Arctic observatory Zeppelin, Atmos. Chem. Phys., 14, 6427-6442, 10.5194/acp-14-6427-

1065 2014, 2014.

1066 Yttri, K. E., Schnelle-Kreis, J., Maenhaut, W., Abbaszade, G., Alves, C., Bjerke, A., Bonnier, N., Bossi,

1067 R., Claeys, M., Dye, C., Evtyugina, M., Garcia-Gacio, D., Hillamo, R., Hoffer, A., Hyder, M., Iinuma,

1068 Y., Jaffrezo, J.-L., Kasper-Giebl, A., Kiss, G., Lopez-Mahia, P. L., Pio, C., Piot, C., Ramirez-Santa-

1069 Cruz, C., Sciare, J., Teinila, K., Vermeylen, R., Vicente, A., and Zimmermann, R.: An intercomparison

1070 study of analytical methods used for quantification of levoglucosan in ambient aerosol filter samples,

1071 Atmos. Meas. Tech., 8, 125-147, 10.5194/amt-8-125-2015, 2015.

1072 Yttri, K. E., Simpson, D., Bergstrom, R., Kiss, G., Szidat, S., Ceburnis, D., Eckhardt, S., Hueglin, C.,

1073 Nojgaard, J. K., Perrino, C., Pisso, I., Prevot, A. S. H., Putaud, J. P., Spindler, G., Vana, M., Zhang, Y.

1074 L., and Aas, W.: The EMEP Intensive Measurement Period campaign, 2008-2009: characterizing

1075 carbonaceous aerosol at nine rural sites in Europe, Atmos. Chem. Phys., 19, 4211-4233, 10.5194/acp-

1076 19-4211-2019, 2019.

1077 Zotter, P., Ciobanu, V. G., Zhang, Y. L., El-Haddad, I., Macchia, M., Daellenbach, K. R., Salazar, G.

1078 A., Huang, R. J., Wacker, L., Hueglin, C., Piazzalunga, A., Fermo, P., Schwikowski, M., Baltensperger,

1079 U., Szidat, S., and Prevot, A. S. H.: Radiocarbon analysis of elemental and organic carbon in Switzerland

1080 during winter-smog episodes from 2008 to 2012-Part 1: Source apportionment and spatial variability,

1081 Atmos. Chem. Phys., 14, 13551-13570, 10.5194/acp-14-13551-2014, 2014.

1082   Zotter, P., Herich, H., Gysel, M., El-Haddad, I., Zhang, Y. L., Mocnik, G., Huglin, C., Baltensperger,

1083   U., Szidat, S., and Prevot, A. H.: Evaluation of the absorption angstrom exponents for traffic and wood

1084   burning in the Aethalometer-based source apportionment using radiocarbon measurements of ambient

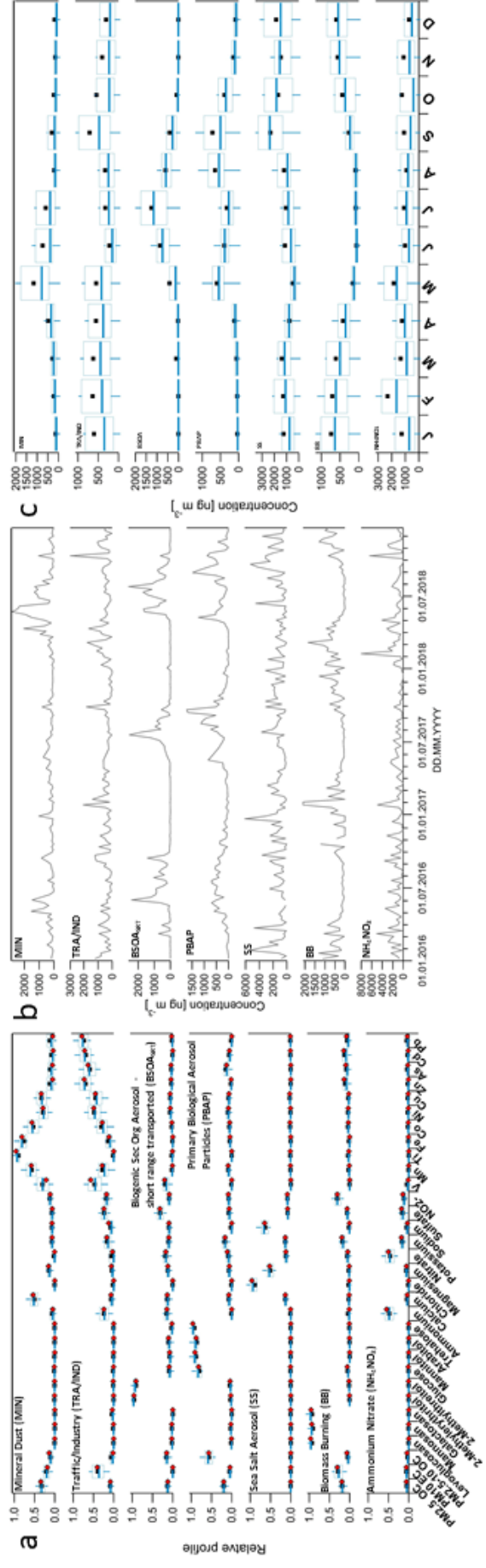1085   aerosol, Atmos. Chem. Phys., 17, 4229-4249, 10.5194/acp-17-4229-2017, 2017.

1086
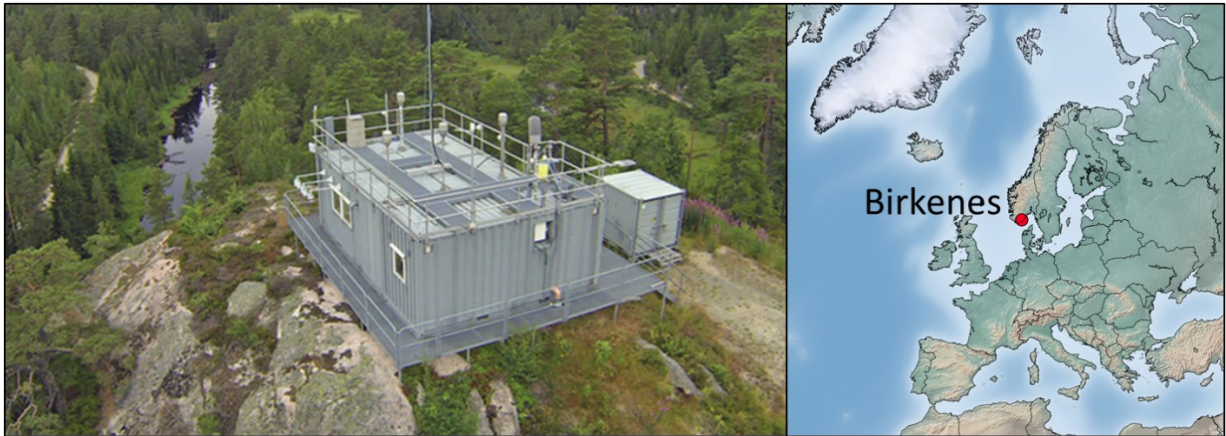
Figures

Figure 1: The Birkenes Observatory (58°23' N, 8°15' E; 219 m asl) lies in the Boreo-nemoral zone, 20 km from the Skagerrak coastline in Southern Norway.

Figure 2: Results from PMF for Birkenes 2016–2018. a) Factor profiles b) Factor time series c) aggregated monthly data. Boxes in a), c) show statistics from bootstrapped solutions (n=5000): percentiles 25/75 (box), median (horizontal line) and 10/90 (whiskers). Black markers are the means. Red markers in a) show the base factor profiles.

Footprint: 30-May-2018 to 06-Jun-2018
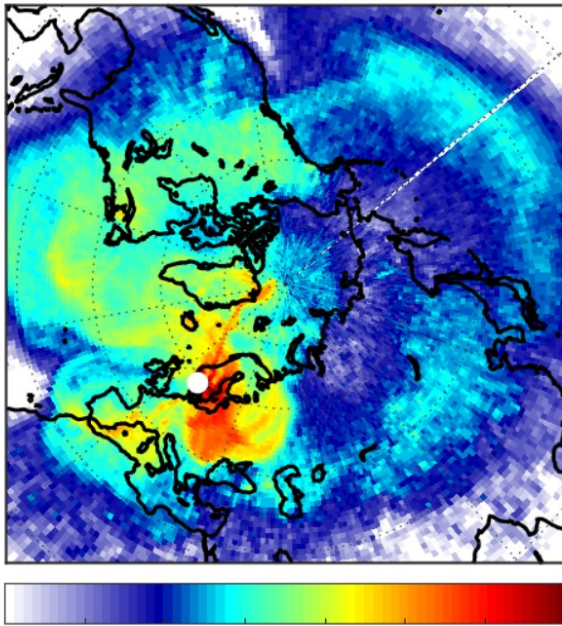
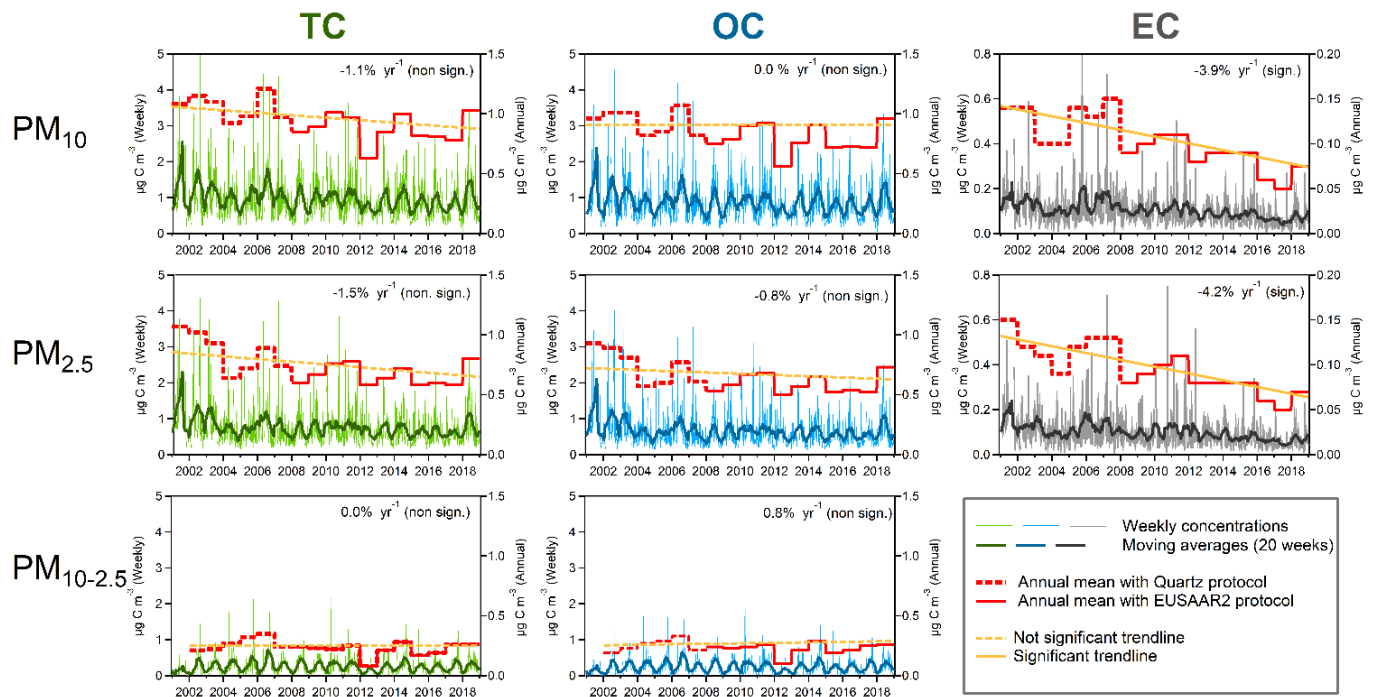0.00 0.00 0.02 0.06 0.25 1.00 4.00 16.00

Averaged emission sensitivity [ns m^{-2}]

Figure 3: Footprint emission sensitivities calculated using the FLEXPART model for the period 30 May–6 June 2018 at the Birkenes Observatory.
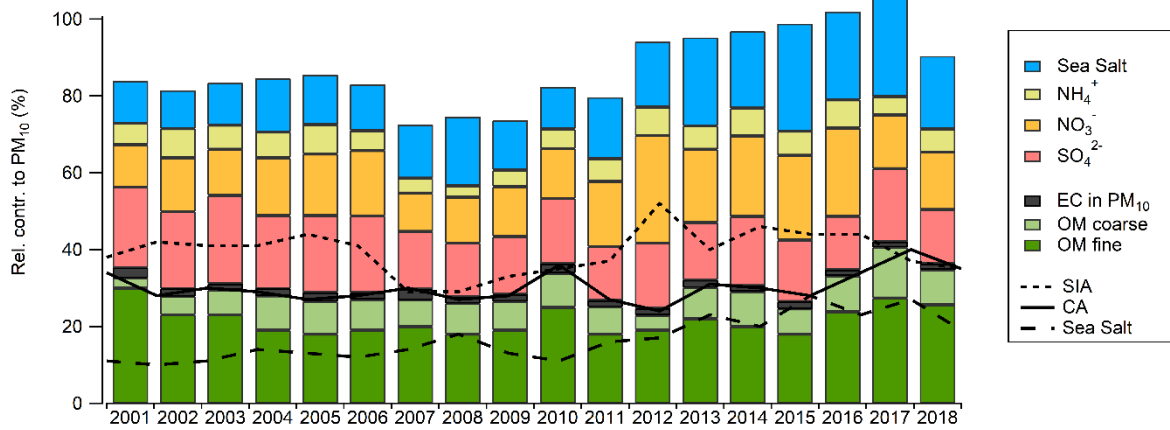
1100

Figure 4: Ambient aerosol concentrations of TC, OC and EC in PM_{10} (Upper panels), in $PM_{2.5}$ (Mid-Panels), and TC and OC in $PM_{10-2.5}$ (Lower panels), presented as weekly (168 h) and annual mean concentrations for the Birkenes Observatory for 2001–2018. The trendlines account for the protocol shift.
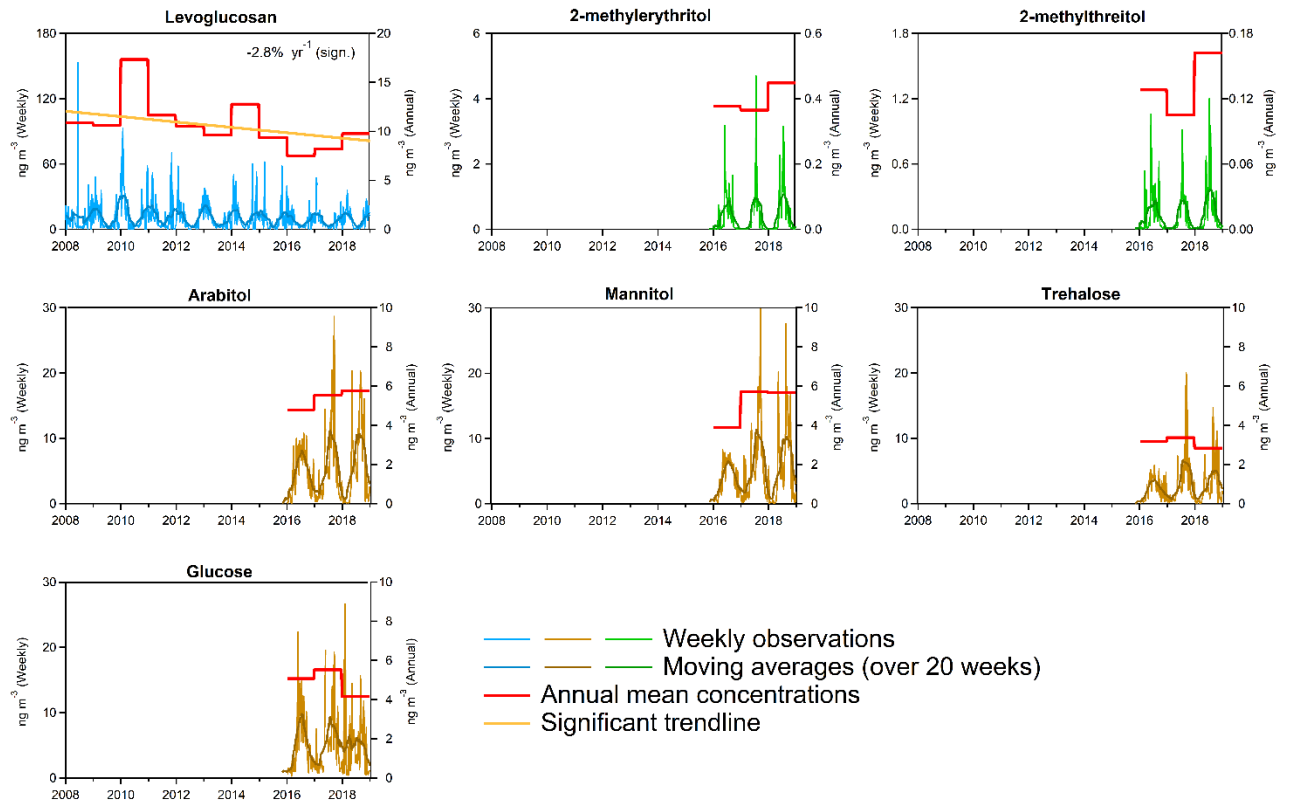
1101
1102
1103

1104

1105

Figure 5: Mass closure of PM₁₀ for Birkenes for the period 2001–2018 (Unit: %). Notation: Sea salt = Sum of Na⁺, Mg²⁺,

Cl⁻; SIA = Secondary inorganic aerosol (SIA) = Sum of SO₄²⁻, NO₃⁻; NH₄⁺; CA = Carbonaceous aerosol; OM = Organic

matter. OM is calculated using OC:OM=1.9 (Yttri et al., 2011a).

1109

1110

Figure 6: Ambient aerosol concentrations of organic tracers in PM$_{10}$. Levoglucosan, 2-methylerythritol and 2-methylthreitol (Upper panels), arabitol, mannitol, trehalose (Mid-Panels), and glucose (Lower panel), presented as weekly (168 h) and annual mean concentrations for the Birkenes Observatory for the period 2008–2018.

1114

a) NDJFM high FF

b) NDJFM high BB

c) MJJAS high FF

d) MJJAS high BB
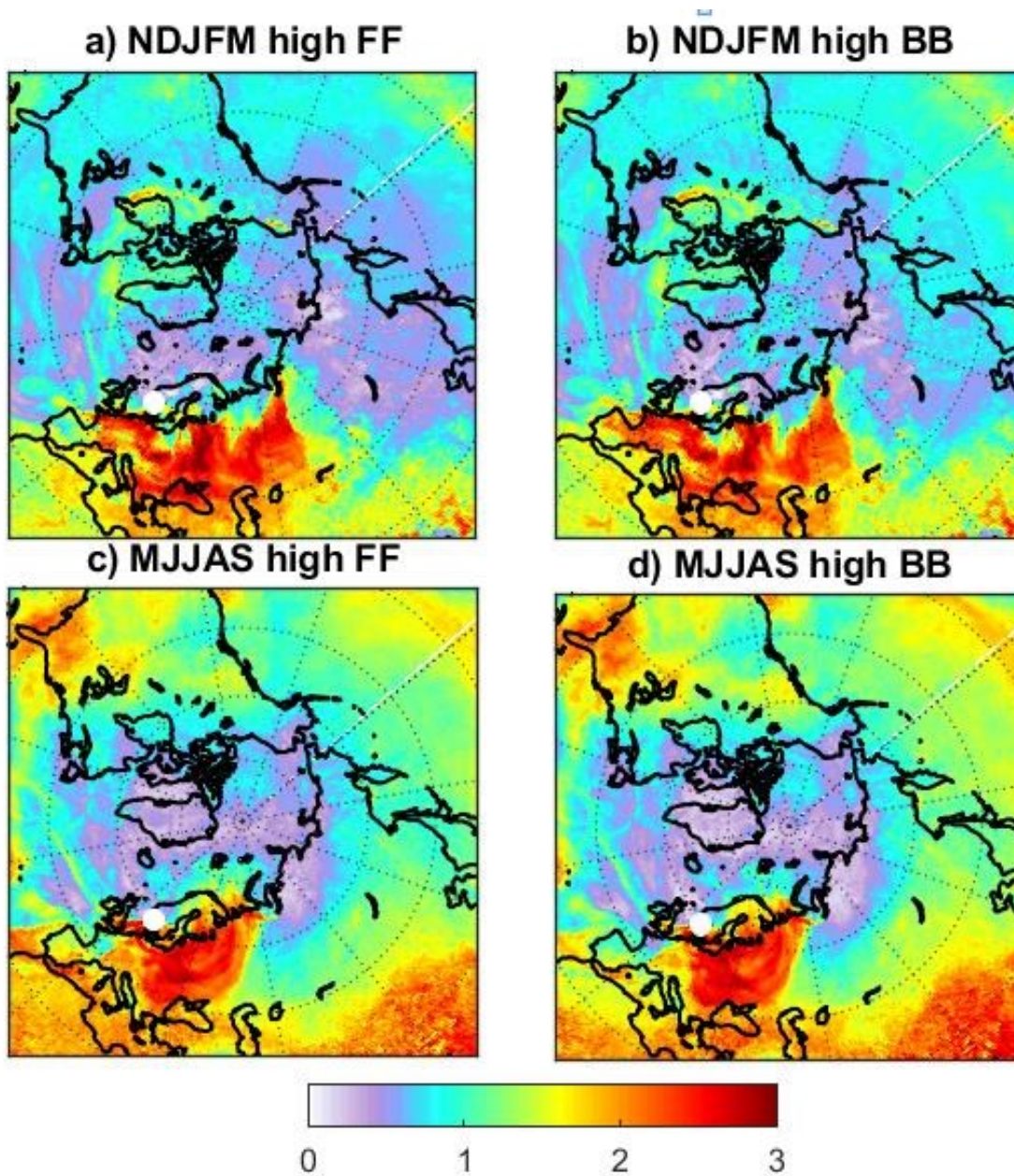
1115

Figure 7: 70th percentiles of eBC$_{ff}$ (left panels, a and c) and eBC$_{bb}$ (right panels, b and d) for winter (NDJFM) and summer (MJJAS). The color-coding shows the ratio of residence times for footprint sensitivities during measurements exceeding the 70th percentile and the average footprint sensitivity.

1116

1117

1118

1119
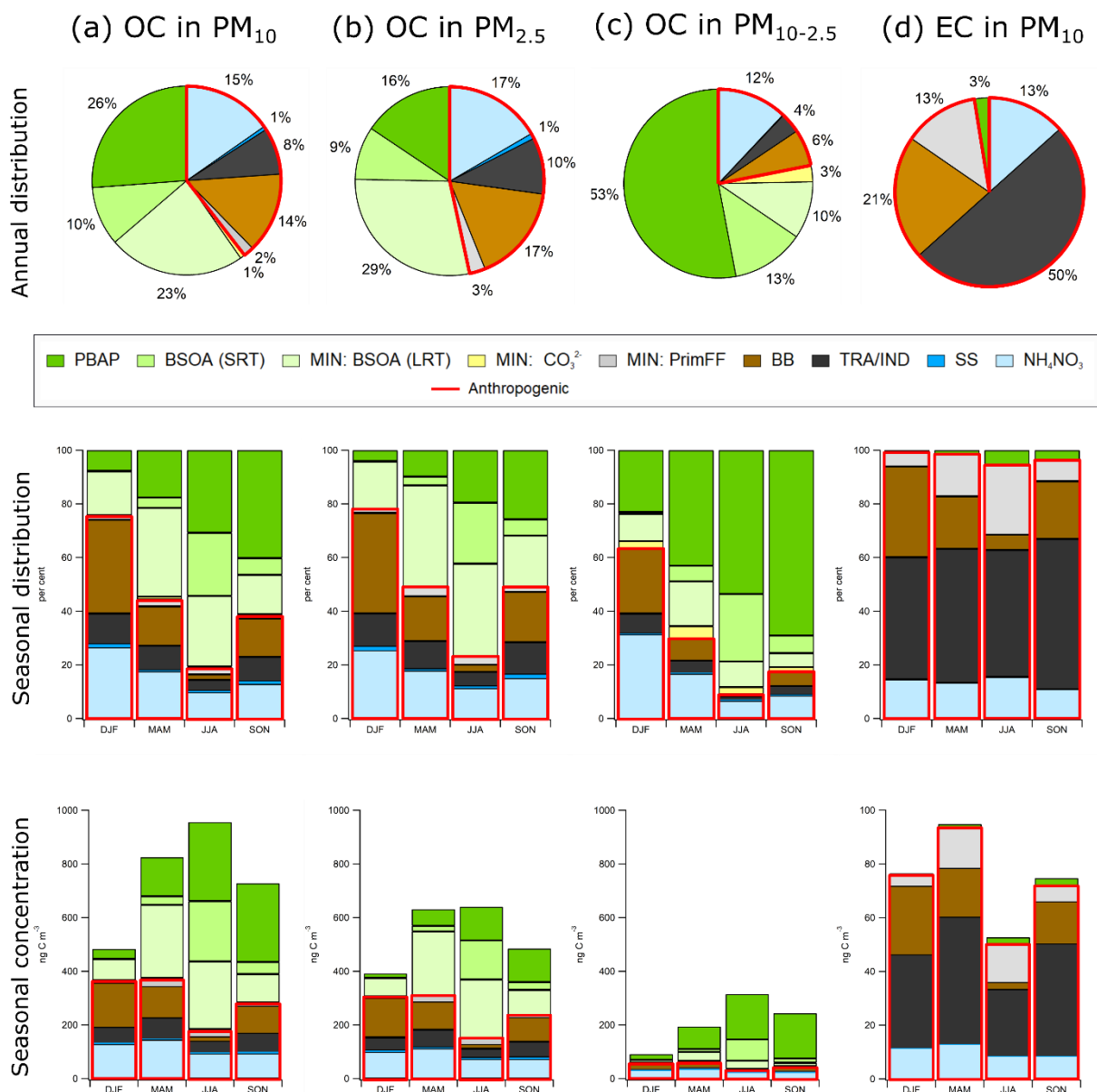
1120
1121 **Figure 8: Factor contributions to OC in PM_{10} (a), $PM_{2.5}$ (b), $PM_{10-2.5}$ (c), and EC in PM_{10} (d) at Birkenes (2016–2018)**
1122 **(upper panels), and divided into seasons (middle and lower panels), as determined by positive matrix factorization. The**
1123 **factors enclosed by the full red line represents anthropogenic sources. The OC content of the MIN factor is divided into**
1124 **long range transported BSOA ($OC_{BSOA,LRT}$) and primary OC from fossil fuel combustion (OC_{PrimFF}) following Eq. (1),**
1125 **and carbonate carbon (OC_{CO32-}) (Sect. 2.4.1).**

1126
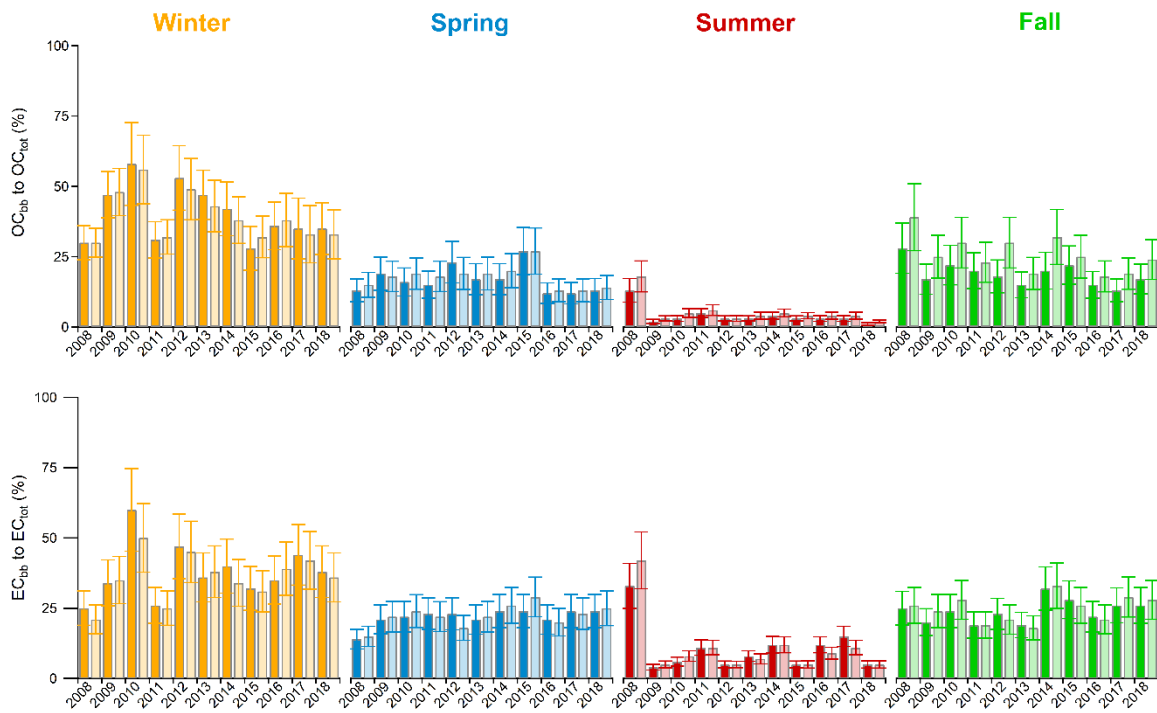
Figure 9: Relative contribution of OC_{bb} to OC_{tot} (upper panel) and EC_{bb} to EC_{tot} (lower panel) in PM_{10} (dark colors) and in $PM_{2.5}$ (light colors), as a function of season at Birkenes for 2008–2018 (DJF = Winter; MAM = Spring; JJA = Summer; SON = Fall).

1132 **Tables**

1133 **Table 1: Variables describing the biomass burning source derived from the PMF BB factor in the present study, and**

1134 **comparable variables obtained by ^{14}C-analysis reported by Zotter et al. (2014).**

Present study	Zotter et al. (2014)[1]
OC/Levoglucosan (in PM_{10}) = 12.7	OC_{NF}/Levoglucosan (in PM_{10}) = 12.6 ± 3.1
OC/Levoglucosan (in $PM_{2.5}$) = 11.1	
EC/Levoglucosan (in PM_{10}) = 1.96	EC_{NF}/Levoglucosan (in PM_{10}) = 1.72 ± 0.59
OC/EC (in PM_{10}) = 6.5	$OC/_{NF}EC_{NF}$ (in PM_{10}) = 7.7 ± 2.1
OC/EC (in $PM_{2.5}$) = 5.7	

1135 [1]North of the Alps

1136 Notation: OC_{NF} = Non-fossil OC; EC_{NF} = Non-fossil EC

1137

1138 **Table 2: Biomass burning fraction derived from the PMF and the aethalometer model. Aethalometer model 1 shows**
1139 **the biomass burning fraction obtained by the default pair of Absorption Ångstrøm Exponents (AAE) suggested by**
1140 **Zotter et al. (2014), whereas Aethalometer model 2 show the biomass burning fraction obtained using the pair of AAEs**
1141 **derived from PMF.**

	PMF	**Aethalometer model 1**	**Aethalometer model 2**
Biomass burning fraction	0.27	0.48	0.28
Fossil AAE	0.93	0.9 (Zotter et al., 2014)	0.93 (from PMF)
Biomass burning AAE	2.04	1.68 (Zotter et al., 2014)	2.04 (from PMF)

1142

1143 **Table 3: OC_{BSOA}, short-range transported (SRT) and long-range transported (LRT), and OC_{PBAP} concentrations and their relative contribution to OC in PM_{10} at Birkenes in August,**

1144 **as obtained by Latin Hypercube Sampling (Yttri et al., 2011b) and by PMF (present study).**

	Reference	Approach	$OC_{BSOA,SRT}$ (ng C m^{-3})	$OC_{BSOA,SRT}$/OC	$OC_{BSOA,SRT+LRT}$ (ng C m^{-3})[2,3]	$OC_{BSOA,SRT+LRT}$/OC[2,3]	OC_{PBAP} (ng C m^{-3})[2]	OC_{PBAP}/OC
August 2009	Yttri et al. (2011b)	LHS[3]			505[1] (408–598)[2,3]	0.48[1] (0.38–0.58)[2,3]	290[1] (213–380)[2]	0.31[1] (0.22–0.40)[2]
August 2016	Present study	PMF	115	0.19	173	0.28	318	0.52
August 2017	Present study	PMF	183	0.19	252	0.26	553	0.57
August 2018	Present study	PMF	159	0.20	316	0.40	287	0.36
August 2016–2018	Present study	PMF	152	0.19	247	0.31	386	0.48

1145   1. 50th percentile
1146   2. 10th–90th percentile
1147   3. LHS-approach includes both $OC_{BSOA,SRT}$ and $OC_{BSOA,LRT}$
1148